Modelling of crystal structures with a significant degree of disorder

Dr Wojciech Andrzej Sławiński

University of Warsaw

Chemistry Department

Pasteura 1 Street

02-093 Warszawa

Summary of research presented in connection with a habilitation application

Warsaw, 1 April 2019

1. **Name**

Wojciech Andrzej Sławiński

2. **Diplomas and graduations obtained – including name, place and year of graduation and the title of the desideration**

Doctor of Philosophy in Physics, Faculty of Physics, University of Warsaw, Warsaw, 28 September 2009, thesis title „Ordering study in manganese oxide $CaCu_xMn_{7-x}O_{12}$ compounds", supervisor prof. R. Przeniosło.

Two semester, postgraduate studies at the Polish-Japanese Institute of Information Technology in Warsaw "Databases and their applications", 7 July 2008.

Master of Science in Physics, specialization *Nuclear Methods in Condensed Matter Physics*, Faculty of Physics, University of Warsaw, Warsaw, 24 June 2004, titled „Magnetic moments reorientation in neodymium orthoferrite studied using neutron powder diffraction", supervisor prof. R. Przeniosło.

3. **Information about employment**

10.2018 – now	University of Warsaw, Faculty of Chemistry, adjunct
10.2015 – 09.2018	Science and Technology Facility Council, ISIS Neutron and Muon Source, Great Britain, Post-Doctoral position
08.2012 – 09.2015	University of Oslo, Centre for Materials Science and Nanotechnology, Chemistry Department, Norway, Post-Doctoral position
02.2010 – 09.2012	University of Warsaw, Faculty of Physics, adjunct
11.2009 – 01.2010	University of Warsaw, Faculty of Physics, scientific and technical specialist

4. **Description of an achievement according to *art. 16 ust. 2 ustawy z dnia 14 marca 2003 r. o stopniach naukowych i tytule naukowym oraz o stopniach i tytule w zakresie sztuki* (Dz. U. 2016 r. poz. 882 ze zm. W Dz. U. z 2016 r. poz. 1311)**

   a. Title of an achievement

Modelling of crystal structures with a significant degree of disorder

b. Publication list being a part of the presented achievement (author/authors, title/titles, publication year, name of the publisher, referees of the publisher)

		IF at the publication year	Number of citations according to Web of Science/Scopus
H1	"Structural arrangement in close packed cobalt polytypes" **W.A. Sławiński**, E. Zacharaki, A.O. Sjåstad, H. Fjellvåg, Crystal Growth and Design, 18 (4), 2018, 2316–2325 My personal contribution was: preparation (application for beamtime at European Synchrotron Radiation Facility, Grenoble, France) and performing diffraction experiments, analysis of collected data, preparing of multiple models of cobalt nanoparticles, performing simulations and refining models against diffraction patterns, manuscript preparation including all figures and charts within the publication. I estimate my contribution at around 75% of the total work	3.972 (2017)	2/2
H2	"Chemical imaging of Fischer-Tropsch catalysts under operating conditions" S.W. Price, D.J. Martin, A.D. Parsons, **W.A. Sławiński**, A. Vamvakeros, S.J. Keylock, A.M. Beale, J.F. Mosselmans, Science Advances, 3, 2017, e1602838 My contribution to the manuscript: analysis of experimental data (powder diffraction patterns), proposing crystal structure models of cobalt nanoparticles, performing simulations and refinements against experimental data, preparation of the manuscript text (part about modelling of disordered crystal structure) and preparation of figure 5 (left and right), analysis of the data shown as Table S2 and S3 (Supplementary Information) and helping with preparation of the manuscript I estimate my contribution at around 30% of the total work	11.511	23/18

H3	"In situ solid-state NMR and XRD studies of the ADOR process and the unusual structure of zeolite IPC-6" S.A. Morris, G.P.M. Bignami, T. Tian, M. Navarro, D.S. Firth, J. Cejka, P.S. Wheatley, D.M. Dawson, **W.A. Sławiński**, D.S. Wragg, R.E. Morris, S.E. Ashbrook, Nature Chemistry 9(10), 2017, 1012 My contribution to the manuscript was: analysis of experimental powder diffraction data, proposing models of IPC-6 crystal structure, performing simulations and refinements of powder diffraction patterns, preparation of the text describing modelling of crystal structure and figure 4 (left and right), discussion of experimental data and its importance to the description of the *assembly–disassembly–organization–reassembly* process, simulation of powder diffraction patterns for different crystal structure models shown on the figure S3 and S5 (Supplementary Information) and help with the manuscript preparation. I estimate my contribution at around 20% of the total	26.201	12/13
H4	"Stacking Faults and Polytypes for Layered Double Hydroxides: What Can We Learn from Simulated and Experimental X-ray Powder Diffraction Data?" **W. A. Sławiński**, A. O. Sjåstad, H. Fjellvåg, Inorganic Chemistry, 55, 2016, 12881-12889 My contribution to the publication was: planning of the experiment (application for beamtime at European synchrotron Radiation Facility, Grenoble, France), performing powder diffraction experiments, analysis of experimental data, preparation of crystal structure models for *Layered-Double-Hydroxides* compounds, performing simulations and refinements of powder diffraction patterns, preparation of the manuscript text and all figures and charts within the publication.	4.857	5/8

	I estimate my contribution at around 80% of the total		
H5	"A novel polytype – the stacking fault based γ-MoO_3 nanobelts" **W. A. Sławiński**, O. Fjellvåg, A. Ruud, H. Fjellvåg, Acta Cryst. B, B72, 2016, 201-208 My contribution to the manuscript covered the analysis of synchrotron radiation-based powder diffraction data, preparation of the crystal structure model of MoO_3 nanobelts, performing Transmission Electron Microscopy and Electro Diffraction experiments, running simulations and refinements of powder diffraction patterns and preparation of all figures and charts within the publication. I estimate my contribution at around 70% of the total	1.887	1/1
H6	"Nanoporous Intergrowths: how crystal growth dictates phase composition and hierarchical structure in the CHA/AEI system" R. Smith, **W. Slawinski**, A. Lind, D. Wragg, J. Cavka, B. Arstad, H. Fjellvåg, M. Attfield, D. Akporiaye, M. Anderson, Chemistry of Materials, 27 (12), 2015, 4205 My contribution to the publication was: analysis of all diffraction patterns, obtaining models of crystal structure of SAPO-18/34 zeolite family using two models of possible disorder models (described in **H7** paper) *Growth* and *Displacement*, structural data analysis as a function of Si content which lead to phase diagram preparation on figure 14 and table 1, preparation of figures 2, 3, 4, 11 and 14, writing of the manuscript text (part about powder diffraction data refinements and modelling of partially disordered structures) and help with the manuscript preparation. I estimate my contribution at around 40% of the total	9.407	17/17

H7	"Intergrowth structure modelling in silicoaluminophosphate SAPO-18/34 family" **W. Sławiński**, D. Wragg, D. Akopriaye, H. Fjellvåg, *Microporous and Mesoporous Materials 195, 2014, 311* My contribution to the manuscript was: planning (beamtime application to European Synchrotron Radiation Facility, Grenoble, France) and performing powder diffraction experiment, analysis of experimental data, preparation of crystal structure models for SAPO-18/34 family members of different possible disorder: *Displacement* and *Growth*, performing simulations and refinements of powder diffraction patterns, establishing quantitative way for disorder level estimation, preparation of publication text and all figures and charts within the manuscript. I estimate my contribution at around 80% of the total	3.453	18/19

c. Description of scientific/artistic goals of above listed work and results obtained including possible applications

Introduction

The main objective of the work presented in this report is to determine the crystal structures of the selected chemical compounds which show characteristic, significant disorder. Also, the aim is to describe the impact of this disorder on the chemical and physical properties of these materials. The term "a *significant degree of disorder"*, should be understood in this work as a persistent deviation from the three-dimensional, periodic structure of the material that makes it impossible to describe its structure and properties without explicitly considering the inherent disorder of the structure.

The crystal structure of a material determines a number of its physical and chemical properties. This means that some physical phenomena occur more frequently in the case of structures with a specific crystal structure. In order to analyse and model material properties, it is crucial to parameterize the atomistic model of a given material in very fine detail.

According to the current definition by International Union of Crystallography (IUCr) [1]

> *„ A material is a CRYSTAL if it has **essentially** a sharp diffraction pattern. The word **essentially** means that most of the intensity of the diffraction is concentrated in relatively sharp **Bragg peaks**, besides the always present diffuse scattering. In all cases, the positions of the diffraction peaks can be expressed by*
>
> $$\boldsymbol{H} = \sum_{i=1}^{n} h_i \boldsymbol{a}_i^* \quad (n \geq 3)$$
>
> *Here $\boldsymbol{a}_i^*$ and h_i are the basis vectors of the reciprocal lattice and integer coefficients respectively and the number n is the minimum for which the positions of the peaks can be described with integer coefficient h_i. The conventional crystals are a special class, though very large, for which n = 3."*

In the classical definition of a crystal, the number of vectors *n* necessary to describe the diffraction pattern was equal to 3. This meant that a material was considered to be a crystal when it had a periodic ordering of atoms in three dimensions. As progress was made in material science, the classic definition had been extended to additionally cover materials where the number of dimensions was n > 3, i.e. modulated crystal structures, quasicrystals or composite crystals. It should also be mentioned that low-dimensional materials (2D and 1D) with a periodic arrangement of atoms in one or two dimensions can also be understood as crystals.

The classical definition mentioned above, defines a crystal as a material that gives a discrete diffraction pattern, even in the presence of diffuse scattering. In the case of partially disordered materials, a significant part of the scattered intensity is observed in between the discrete Bragg peaks. In such cases this part of the scattered radiation is indeed an important contribution to the full diffraction pattern and should be considered during the analysis of experimental diffraction data. A characteristic feature of the diffraction patterns of partially disordered materials is that they consist of two, equally important, contributions: narrow diffraction maxima and diffuse intensity away from the maxima, which, indeed cannot be omitted in analysis of the diffraction data. The analysis of this second contribution allows one to discover unknown structural features of the material. It is therefore difficult to say whether the definition of a crystal includes materials that are the subject of this work, or perhaps this definition should be extended.

What are than partially disordered materials? These are materials whose structure can be described in terms of two-dimensional layers. These layers are fully periodic sets of atoms, of a thickness much smaller in its third dimension than the other two. The diffraction pattern of such two-dimensional layer would be a collection of discrete points. The three-dimensional space of the material can therefore be filled with two-dimensional layers in many ways. The distance between the two consecutive layers, the relative translation between the layers, as well as the sequence in which these layers occur are all crucial details that determine the resulting diffraction images. It is of course possible to fill the three-dimensional space with two-dimensional layers such that they will be arranged in a periodic manner (in 3D). In such a case, the diffraction image will mainly consist of discrete diffraction maxima, *i.e.* the material will have a crystalline, periodic structure (according to the definition given above).

However, there are also many possible arrangements (sequences) of two-dimensional layers in which the translational symmetry will not be conserved in a direction perpendicular to the layers. In these cases, the diffraction pattern will be the sum of many discrete diffraction maxima derived from the fully periodic two-dimensional layers and also include contributions from broad, diffuse scattering maxima. It is also worth mentioning, one more possibility. When two-dimensional layers are arranged in a periodic manner there exist the probability of defects (mistakes) in the arrangement of the layers. This means that the area within the crystal (in a direction perpendicular to the layers) that scatters coherently is significantly decreased. This

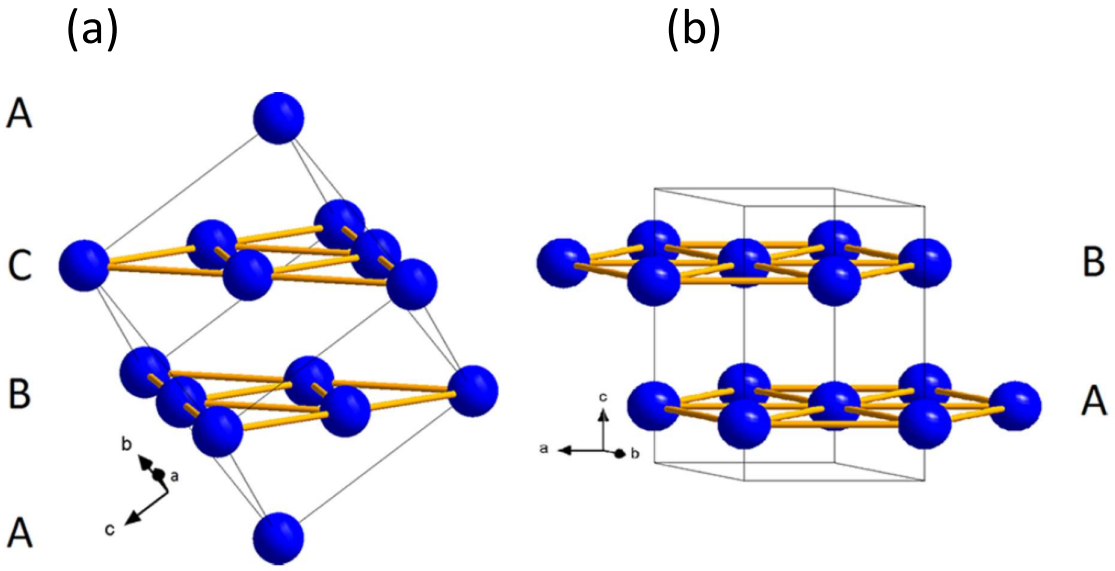

Figure 1 Unit cells of cubic closed pacjed *ccp* (left) and hexagonal closed packed *hcp* (right) crystal structures. The *ccp* unit cell is rotated to make [111] direction parallel to [001] direction in the *hcp* unit cell. The connected atoms show the hexagonal close-packed planes, which are here considered as the key building units (layers). (Figure taken from paper **H1**).

results in a significant broadening of the diffraction maxima in one direction. This broadening of these diffraction peaks is closely related to the probability of faults in the arrangement of two-dimensional layers.

The description of the structure of partially disordered materials (as presented above) will be illustrated by an example from the paper **H1** - nanoparticles of metallic cobalt. This material can crystallize in two related structures (it has also other crystalline forms). The first one is the *cubic closed packed (ccp)* structure, the second is the *hexagonal closed packed* (hcp) structure. The *ccp* structure is described in cubic, face-cantered lattice in the space group $Fm\bar{3}m$, while the *hcp* in the hexagonal lattice, in the space group $P6_3/mmc$. Figure 1 shows these two structures. The unit cells have been rotated in such a way as to show that both structures can be described in terms of identical layers.

Both structures are shown in Figure 1. The hexagonal crystalline layers are arranged in a fully periodic manner. Letters A, B and C denote the position of the respective layers. In the case of the *ccp* structure, the layers are arranged in such a way that they create a sequence of ABCABC ..., while in the case of the *hcp* structure, the sequence is ABABAB ... In both cases the layers are arranged in a periodic manner so the diffraction pattern in both cases was

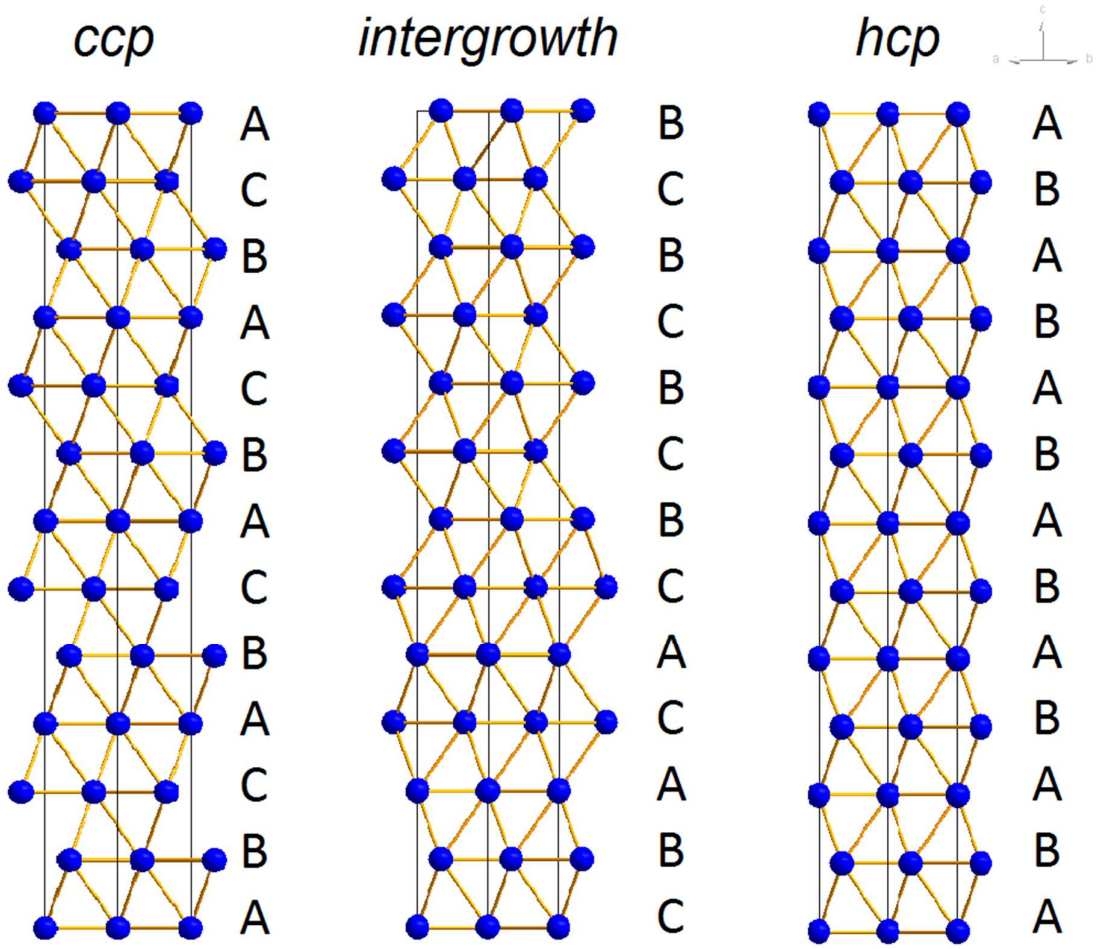

Figure 2 Three examples of cubic closed packed *ccp*, stacking faulted (intergrowth), and hexagonal closed packed *hcp* crystal structures represented in terms of stacked layers. The *ccp* and *hcp* structures are built with sequences of ABC... and AB..., respectively. The stacking faulted intergrowth structure is built with a fully random sequence. (Figure taken from paper **H1**).

composed by a set of sharp Bragg maxima. Diffuse scattering would have a small effect, and it would mainly be caused by the thermal vibrations of atoms.

Any fault in the periodic sequence of layers will break the translational symmetry in the direction perpendicular to the layer. In the case of a small probability of faults in the stacking, we can consider faults as defects in the crystal. Due to these defects one can observe broadening of the Bragg maxima. The probability of defects occurring will define the width of this broadening.

In cases where the periodic sequence of layers is disturbed significantly, for example when the probability that after layers AB the layers A or C will occur with equal probability (50% for A and 50% for C), it is no longer possible to describe the structure in terms of structural defects. In this situation, the material's characteristic structural feature is its random nature. And only

by taking into account this random character is it possible to precisely characterize the material.

Figure 2 shows three crystalline structures which have different arrangements of two-dimensional layers: the *ccp* structure (left), the structure of randomly stacked layers (middle) and the *hcp* structure (right). The structure presented in the middle of Figure 2 is only one of many possible representations in which the layers are stacked one after the other in a random sequence. In the example in Figure 2, the crystal is comprised of the sequence of BCBCBCBCACABC... One can see that there are regions corresponding to two periodic structures *ccp* and *hcp*. However, these fully periodic regions are just a few layers thick. Therefore, the regions of coherent scattering in such crystals are not too large. In these cases, the diffraction pattern is the sum of discrete Bragg reflections coming from periodic, two-dimensional, crystalline layers and wide diffuse maxima originating from smaller areas characteristic for the *ccp* and *hcp* structure.

As mentioned above, the structure of materials can be studied, with great success, using diffraction techniques as was discovered by M. von Laue [2], and described in detail by W.H and W.L Bragg in 1913 [3]. Bragg's law forms the basis of all diffraction experiments, carried out using X-rays, synchrotron radiation and neutrons. The following formula by W.L. Bragg describes the required condition for the diffraction on the crystal to occur

$$2d_{hkl}\, sin\, \theta = n\lambda$$

where d_{hkl} is the distance between the atomic planes, θ is the half the angle between the incident and scattered beam, n is the natural number and λ is the wavelength of the radiation used. The fulfilment of Bragg's law is a compulsory condition but is not sufficient to observe the scattered intensity at an angle of 2θ in relation to the incident beam.

In principle, there are two main diffraction methods. Diffraction on single crystals, where the sample has the form of a single crystal, and powder diffraction, where the sample is in the form of a powder consisting of many crystallites. In this work, all studies were carried out using the second method. The basic assumption in the case of powder diffraction method is that the crystallites in the sample are randomly oriented in space. This means that the Bragg condition is met not for a single direction in space, but for the entire cone with a vertical angle of 4θ. The powder diffraction method describes the average structure out of many crystallites present in the sample. Thus, the obtained result gives an average crystal structure, including, potentially, the distribution of crystal parameters as compared to single crystal diffraction).

The intensity of the scattered intensity of Bragg diffraction is proportional to the square of the structure factor F_{hkl}. The structure factor F_{hkl} is calculated as

$$F_{hkl} = \sum_{i=1}^{n} f_i(Q) e^{2\pi i(\boldsymbol{r}_i \boldsymbol{Q})}$$

where **Q** is a scattering vector which, according to Bragg's law, is equal to $\boldsymbol{Q} = h\boldsymbol{a}^* + k\boldsymbol{b}^* + l\boldsymbol{c}^*$, where $\boldsymbol{a}^*, \boldsymbol{b}^*$ and $\boldsymbol{c}^*$ are the unit vectors in the reciprocal space, and *h*, *k* and *l* are the Miller indices of atomic planes in the crystal. $f_i(Q)$ is the atomic scattering form factor or, in the case of neutron scattering, is replaced by the scattering length b_i. $\boldsymbol{r}_i$ is the position of the atom *i* in the unit cell. The summation runs over all *n* atoms in the unit cell. It is worth mentioning here that because a perfect crystal is a periodic structure, summation over atoms in the single unit cell is sufficient. An important difficulty for partially disordered materials is that in this case, the unit cell cannot be determined, because the translational symmetry is broken in the direction perpendicular to the crystalline layers. In such a case, it would be necessary to run the summation over all the atoms in the crystal, which is impossible for obvious reasons.

For small crystals (so-called nanocrystals) less than 20 nm in size, the Debye equation can be used to calculate the powder diffraction pattern:

$$I(Q) = \sum_{i=1}^{n} \sum_{j=1}^{n} f_i(Q) f_j(Q) \frac{\sin \boldsymbol{Q}\boldsymbol{r}_{ij}}{\boldsymbol{Q}\boldsymbol{r}_{ij}}$$

where $\boldsymbol{r}_{ij}$ **i**s the distance between the atoms *i* and *j*. By using the Debye equation, it is possible to model any shape of crystallites and any distribution of atoms in the crystal (any, here also non-periodic). It allows modelling of various effects and defects in the structure, including stress, crystallite shapes and disorder. An important limitation for the use of the Debye equation is that it is required to sum over all the atoms in the crystal twice. This means that calculations for crystallites containing a large number of atoms are impossible, due to the large time needed for calculations. But this calculation method is ideal for nanomaterials.

In the case of large crystallites, the basic method of analysing data obtained from X-ray, synchrotron radiation or neutron powder diffraction is the Rietveld method [4]. First described in 1969 by Hugo Rietveld, it allows one to simulate a powder diffraction pattern by calculating the structure factor F_{hkl} for all atomic planes in a crystal, and then multiplying these intensities by a function which describes the shape of the Bragg peak. Once several other corrections and apparatus factors are considered, it is possible to compare the calculated diffraction pattern with experimental data. Then, by using the least square method, it is possible to find a global minimum for parameters describing the structure of the material and other instrumental parameters. The main limitation for the use of the Rietveld method is that it can only be applied to periodic structures, where it is sufficient to sum over all the atoms in the unit cell when calculating the structure factor F_{hkl}.

In the case of materials when it is important to take into account faults in the arrangement of crystalline layers or their random arrangement, it is necessary to modify the procedure for the calculation of powder diffraction patterns. Instead of calculating the structure factor F_{hkl} as a sum over all the atoms in the crystal, the property of Fourier transform can be used. Which is that the Fourier transform of the convolution of the two functions is the product of the Fourier transforms of these functions. This means that it is possible to separate the Fourier transform for atoms in a single layer, and then multiply this function by a Fourier transform of a function which describes the relative translations of these layers. Moreover, it is not necessary to consider the infinite number of two-dimensional layers until the periodicity within the layer is conserved. It is than possible to limit the calculation to a single unit cell which one can use to build an infinite layer. The Fourier transform calculated for the unit cell of the layer is equal to zero everywhere except for the points ($ha^* kb^* zc^*$) in the reciprocal space. The h and k are integer Miller indices, and z is a real number. The Fourier transform of the function which describes the relative positions of the layers is a continuous function. As a result of multiplying these two Fourier transforms, we obtain the calculated intensity only at points ($ha^* kb^* zc^*$) in the reciprocal space. In order to obtain a powder diffraction pattern, it is only required to project the calculated intensities into a two-dimensional space: the intensity as a function of the scattering vector length Q, or the scattering angle 2θ.

The method described above, allows a significant reduction of the time needed to perform calculations for powder diffraction patterns. The summation runs over all atoms in the unit cell of the layer. On the other hand, it is not possible, as in the case of the Rietveld method, to use the least squares method to find the global minimum for parameters describing the material's structure and instrumental parameters. It is necessary to use a different algorithm, the so-called *evolutionary algorithm*. The evolutionary algorithm generates many sets of parameters which are later used to calculate the powder diffraction patterns. Then all the calculated patterns are compared with experimental datasets. In the next iteration, new sets of parameters are generated by modifying the ones that gave the best fits in the previous step. After carrying out many iterations of this procedure, it is possible to reach a minimum. With a proper selection of the parameters for the entire procedure, it can be assumed that this minimum is a global minimum. This method allows calculations and modelling of powder diffraction patterns for partially disordered structures. However, it is necessary to use high-performance computing clusters, in principle allowing one to perform calculations on many threads at the same time.

The calculation method described above has been implemented in the *Discus* program [4]. It allows, among other capabilities, calculations and refinements of powder and single crystal diffraction patterns, for structures with a significant level of disorder. An *evolutionary algorithm*

is also available in the program. This allows one to search for the best parameters describing the crystal, its disordered structure, and other instrumental parameters. Although *Discus* is a freely available program, is not commonly used for partially disordered materials. Most probably this is due to the complexity of the calculations themselves, or difficulties in using the program. The knowledge of the method used to analyse partially disordered structures is one of my unique skills. This enabled me to establish collaborations with several research groups including:

- the group of prof. H. Fjellvåg, Department of Chemistry, Oslo University, Norway;
- the group of prof. A. Beale, Research Complex at Harwell, Rutherford Appleton Laboratories in Harwell, Didcot, Great Britian;
- the group of prof. R. Morris, EaStCHEM School of Chemistry, University of St Andrews, Great Britian;
- prof. R. Neder, Department of Condensed Matter Physics, Friedrich-Alexander University of Erlangen, Germany.

In order to illustrate the characteristic features of diffraction patterns of partially disordered materials, I calculated the powder diffraction patterns for the three structures shown in Figure 2: two structures that were periodic in three dimensions *ccp* and *hcp*, and one structure which was comprised of randomly stacked layers. Figure 3 shows powder diffraction patterns calculated using radiation of wavelength $\lambda = 0.50486$ Å. In the case of the structure with a random order of layers, one could observe the characteristic features of such diffraction patterns: asymmetric peak shape of the diffraction maxima, anisotropic, *hkl*-dependent broadening of the diffraction peaks and also the disappearance of selected reflections. A significant part of the scattered intensity is observed in between the Bragg peaks. It can be clearly seen that it is necessary to analyse the intensity in the whole range of scattering angles, and not only those derived from the Bragg peaks.

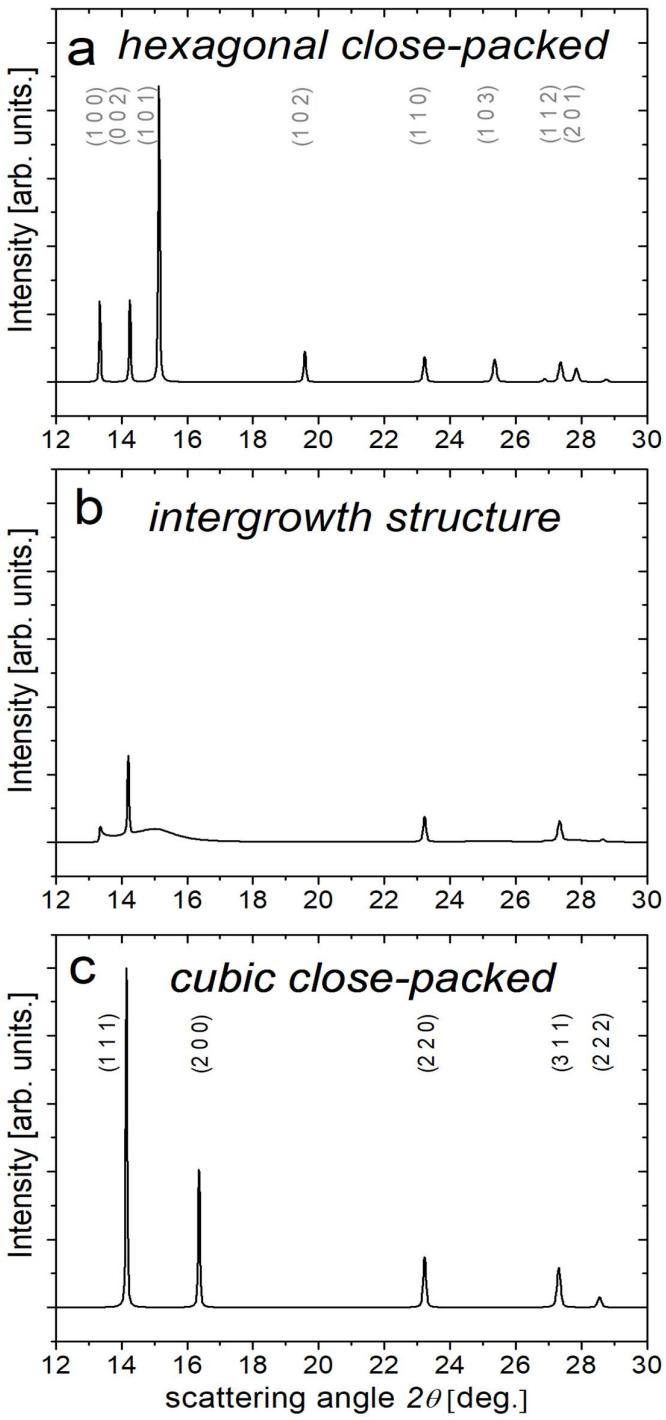

Figure 3 Powder diffraction patterns calcated for three structures: hexagonal closed packed *hcp* (panel a), random staking of hexagonal layers (panel b) and cubic close packed strcutre (panel c).

The calculated diffraction patterns for the *ccp* structure and structures containing stacking faults with a probability from 2 to 10% are shown in Figure 4. One can observe that even the probability of stacking faults a low as 2% in the structure gives a significant broadening of the selected Bragg peaks. For example, the (200) peak is broadened in such a way that its value at its maximum decreases by half (approximately) as compared to the structure without stacking faults. This means that even if a single fault in the layer stacking occurs, on average, once every 50 layers, this feature should be taken into account in order to determine the structure of the material accurately.

The main achievement within the summary presented here, is to use the above-described method of calculating and modelling the structure parameters of partially disordered materials to develop models of crystal structures of selected materials, all of which are characterized by the presence of various defects types, disorders or reduced dimensionality. The construction of accurate models of the crystal structure, which considers the

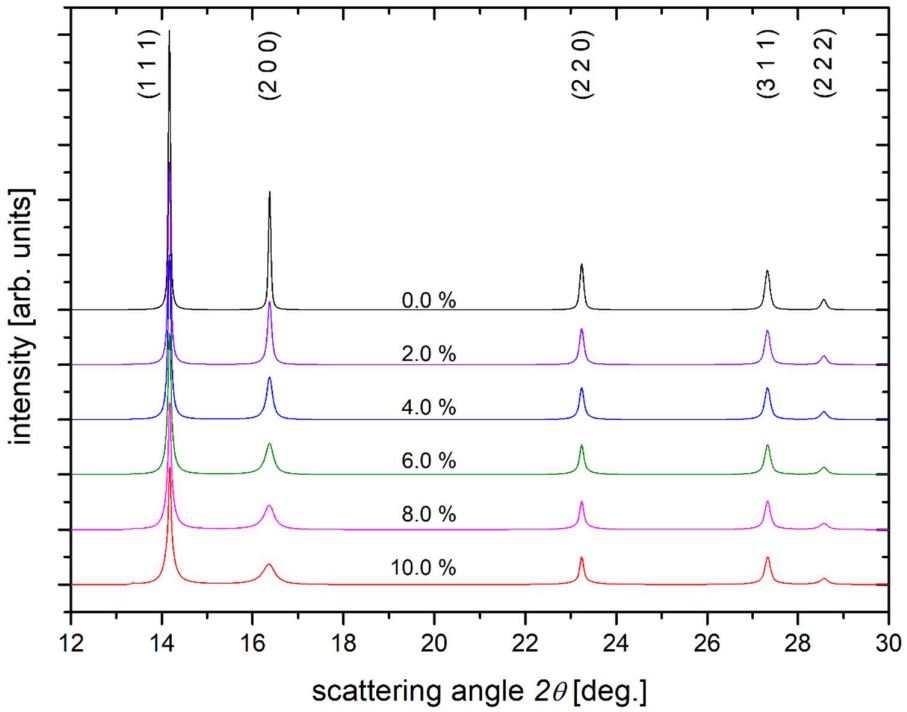

Figure 4 Series of simulated X-ray powder diffraction patterns for cubic closed packed *ccp* structures with 0 to 10 % of stacking fault probability for Co nanoparticles by means of the large particle approach. (Figure is bases on the data from paper **H1**).

disorder in the crystal structure, makes it possible to better understand the physical and chemical properties of these materials.

Results and discussion

Below I present a summary of my results obtained while using the method of calculation powder diffraction patterns (as presented above), published within the papers **H1-H7**. These results concern various seemingly unrelated materials. A key element connecting them is that in order to describe their structure and properties accurately, it is essential to include the partly disordered nature of those materials.

The first sub-group of materials described in the current summery are the crystalline materials in the form of nanoparticles. Due to the small size of crystallites, their properties may significantly differ from the properties of bulk materials. I have described the results on nanomaterials in the papers **H1** and **H2** for cobalt nanoparticles and in the paper **H5** for MoO_3 nanobelts.

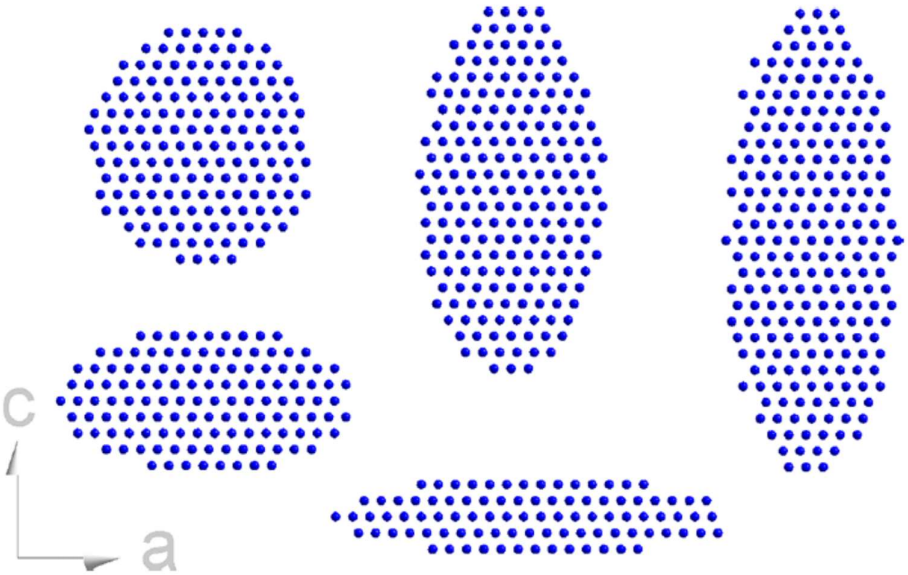

Figure 5 Different Co nanoparticle shapes used for calculations: spherical (top left) and various ellipsoidal anisotropic shapes. Projection along the b-direction visualizes the stacking faults along the c-direction. (Figure taken from paper **H1**).

Nanoparticles of cobalt (nCo) are an interesting material with potential technological application in catalysis [5] or information storage [6]. An important application of these nanoparticles is their use in the Fisher-Tropsch process [7, 8] which is a hydrocarbon formation reaction that uses a mixture of carbon monoxide and hydrogen as starting materials while products are liquid fuels free of sulphur and nitrogen. There are many factors affecting the effectiveness of the Fisher-Tropsch process such as the starting and catalyst material used. The efficiency of the catalyst depends on its crystal structure, order/disorder and substrate type or properties [9]. In order to optimize the catalysis process, it is necessary to understand and describe, in more details, the structure of the material used as a catalyst [10]. There are many research groups working on the theoretical [11, 12] and experimental aspects of this subject [13, 14].

The structure of cobalt nanoparticles has already been described in the introduction to this summary as an example of a possible stacking order of hexagonal layers (Figure 2), including the structure of randomly stacked crystalline layers (Figure 2, middle). In the manuscript **H1** I presented a detailed analysis of the various aspects of deviation from the three-dimensional periodic crystal structure for two possible cases: small nanoparticles (smaller than 20 nm) and large nanoparticles (above 20 nm). This differentiation was required due to the fact that two different calculation methods have been used: the Debye equation (for small nanoparticles)

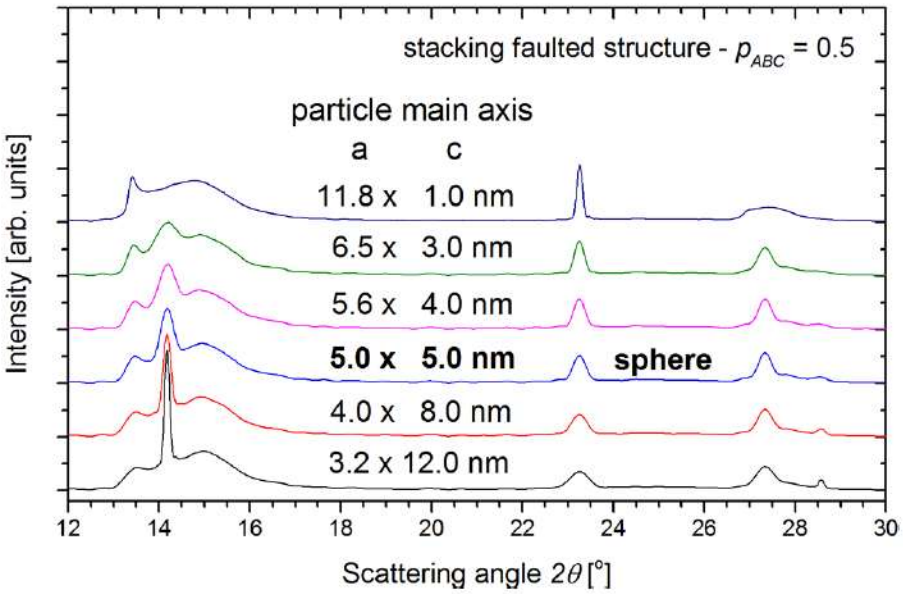

Rysunek 1 Series of simulated X-ray powder diffraction patterns using the Debye scattering equation for ellipsoidal nanoparticles. The relevant pattern for spherical particles is labeled in the middle of the set. All considered particles are fully intergrowth *ccp-hcp* (p_{ABC} = 0.5). λ = 0.50486 Å. (Figure taken from paper **H1**).

and the method used in the *Discus* program (for large nanoparticles). The limited use of the Debye equation comes from the long times required for calculations (proportional to n^2, where *n* is the total number of atoms in the model used). In **H1**, , I presented the results of calculations for a number of parameters modifying the structure, such as disorder in the arrangement of crystalline layers, size of spherical crystallites, crystal size distribution, anisotropic shape of particles and strain (by strain one should understood the shortening or elongating interatomic distances in the nanoparticle in one direction), focusing on small nanoparticles. One of the analysed cases concerned the influence of the anisotropic shapes of crystallites on their diffraction patterns. Figure 5 shows examples of the nanoparticles used for these calculations.

It is usually assumed that there are two main factors that cause the broadening of Bragg diffraction peaks: stress and the sizes of crystallites (Williamson-Hall method) [15]. In the case of partially disordered materials, an additional factor which should be considered is the presence of disorder. Only when taking into account this component the structure can the material be described in detail. Figure 6 presents a series of diffraction patterns, calculated using crystal structure models which explicitly consider both the anisotropic, elliptical nanoparticle shape as well as the stacking faults in the structure. It is plainly visible how important it is to include both effects in order to describe the diffraction pattern give rise to a significant systematic error.

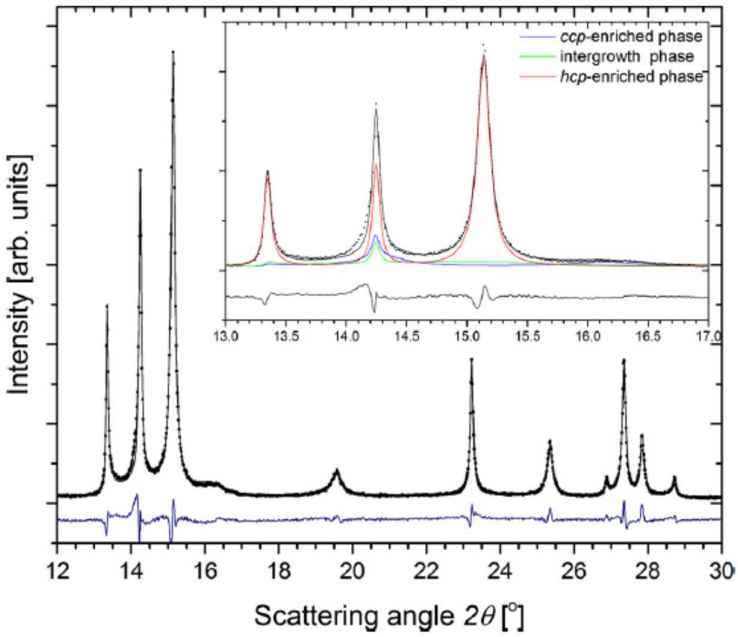

Figure 7 Whole pattern refinement of nano Co samples exposed to He at room temperature. In addition to the observed (points) and calculated patterns (solid, black line), the difference curve is shown below. The inset shows an enlarged view of the low angle part of the measured and calculated patterns, deconvoluted into the contributions from the three constituents, *ccp*-enriched, intergrowth, and *hcp*-enriched. λ = 0.50486 Å (Figure taken from paper **H1**).

In the case of large crystallites, it is not possible to take into account the size nor shape of the crystallites in direct way. Use of the Debye equation is also not possible, due to the significant computing time required. In order to include the structural disorder of crystalline layers, I used the calculation method available in the *Discus* program. Several examples of simulated diffraction patterns are shown in Figures 3 and 4 of the *Introduction* for this calculation method. Incorporating the disorder in the structure allows one to describe the intensity of scattered radiation observed in between the Bragg peaks. It is also worth noting that the diffraction pattern calculated for the structures of material with stacking faults is not a simple linear combination of two diffraction patterns for periodic *ccp* and *hcp* structures.

An important part of the results presented in the work **H1** is the application of the modelling method for large crystallites to be experimentally measured *in-situ* to generate powder diffraction data, *i.e.* in experimental conditions similar to those in the Fisher-Tropsch process. For the purposes of this experiment, measurements were performed for two samples of cobalt nanoparticles, with different initial phase compositions, as a function of temperature for three different gas atmospheres: CO, in comparison to He and H_2. Based on the measured diffraction patterns, I observed that in order to describe those materials in details, it is necessary to think

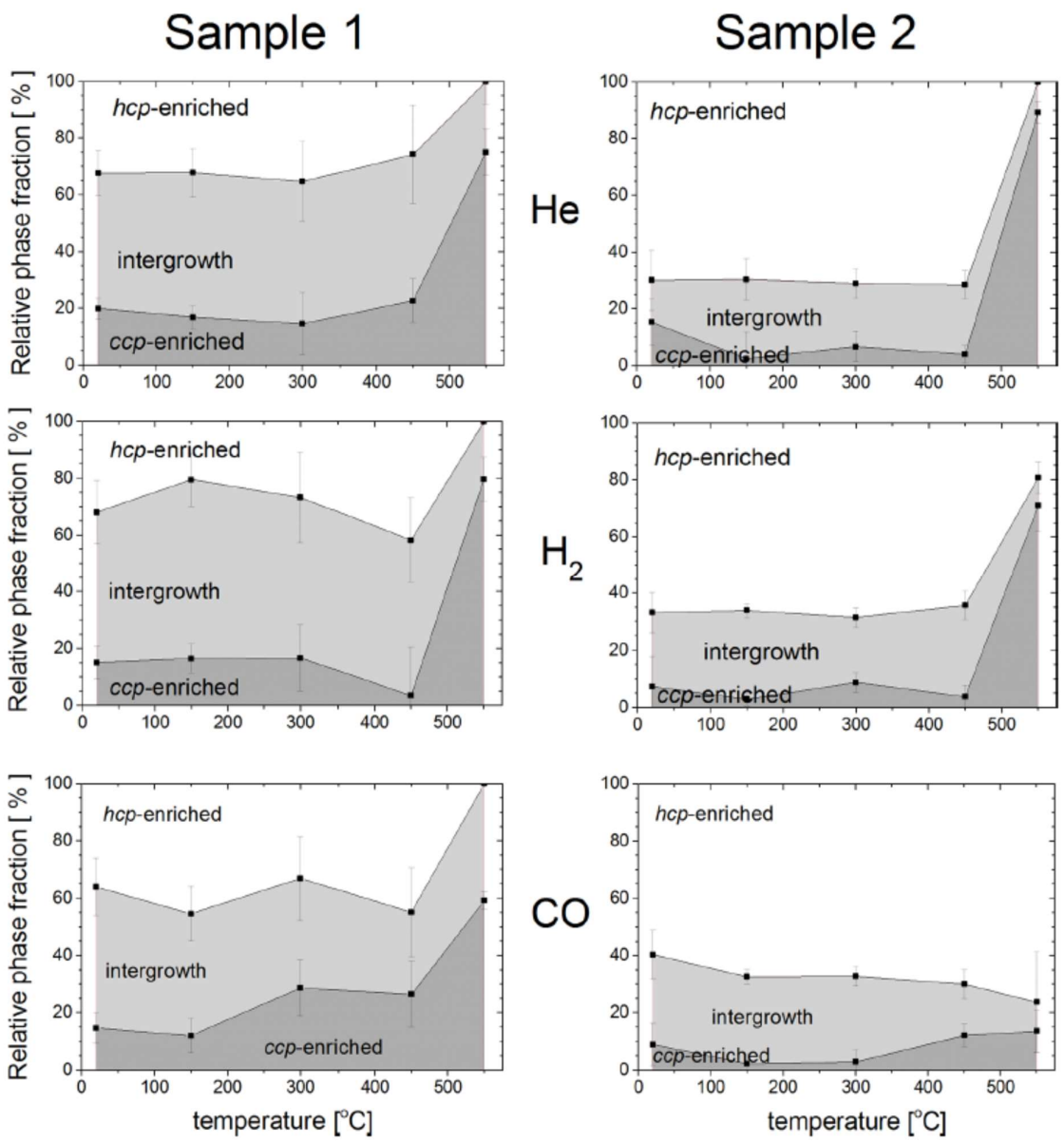

Figure 8 Evolution of *ccp*-enriched, intergrowth, and *hcp*-enriched fractions with temperature and atmosphere (He, H2, CO) for Sample 1 (left panel) and Sample 2 (right panel) (Figure taken from paper **H1**).

about them as being composed of three crystalline phases: one close to the *ccp* and *hcp* portions of the structure (with a slight probability of defects), and a structure with a random sequence of layers (an intergrowth structure). Figure 7 shows the observed diffraction patterns along with simulated diffractograms for the three crystalline phases. As a result of the model evaluation, I obtained a phase diagram of the studied cobalt nanoparticles as a function of temperature, for three gas atmospheres (CO, He and H_2). The dependencies for the two materials vary a lot for each of the atmospheres, in particular for the case of a CO, the

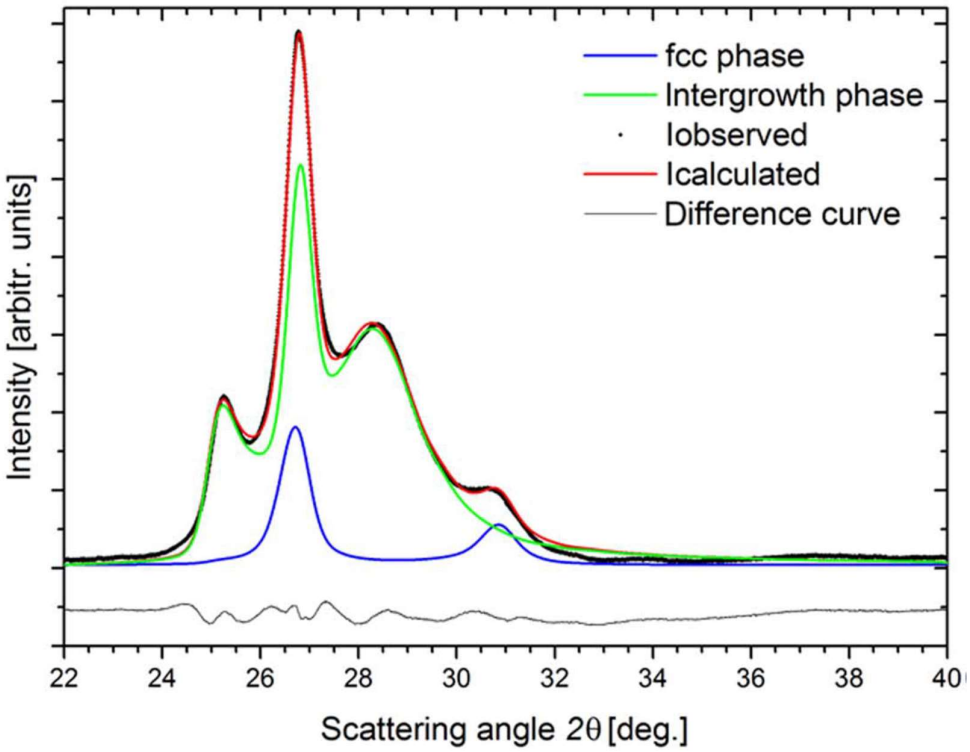

Figure 9 Exemplar fit of the X-Ray powder diffraction pattern generated from cluster analysis of inverse catalyst after reduction using *Discus* program. Black points, experimental pattern; red, fitted pattern; blue, fit to cubic phase; green, fit to intergrown phase; gray, difference curve (figure taken from paper **H2**).

intergrowth phase fraction decreases less prominently. Figure 8 shows phase diagrams as a function of temperature for the two materials investigated.

The methodology of modelling for cobalt nanoparticles in the case of large crystallites presented in detail in the work **H1** was then used to analyse the diffraction data obtained *in-situ* under Fisher-Tropsch process conditions, as presented in paper **H2**. The key achievement of the diffraction experiment as described in **H2** is to use tomographic reconstruction for a real catalyst sample during the catalytic process. This means a series of powder diffraction patterns have been collected as a function of their position in the sample (including the rotation of the sample). Thanks to the use of the tomography method, after reconstruction (processing) of the measured diffractograms, it was possible to obtain diffraction patterns for the individual regions of the sample. This allowed us to separate the areas of interest with different crystal structures: substrate (two phases) along with two separate phases of cobalt nanoparticles. This gave a three-dimensional model of the sample under consideration. I have analysed powder diffraction patterns characteristic of different regions of the sample using the methods

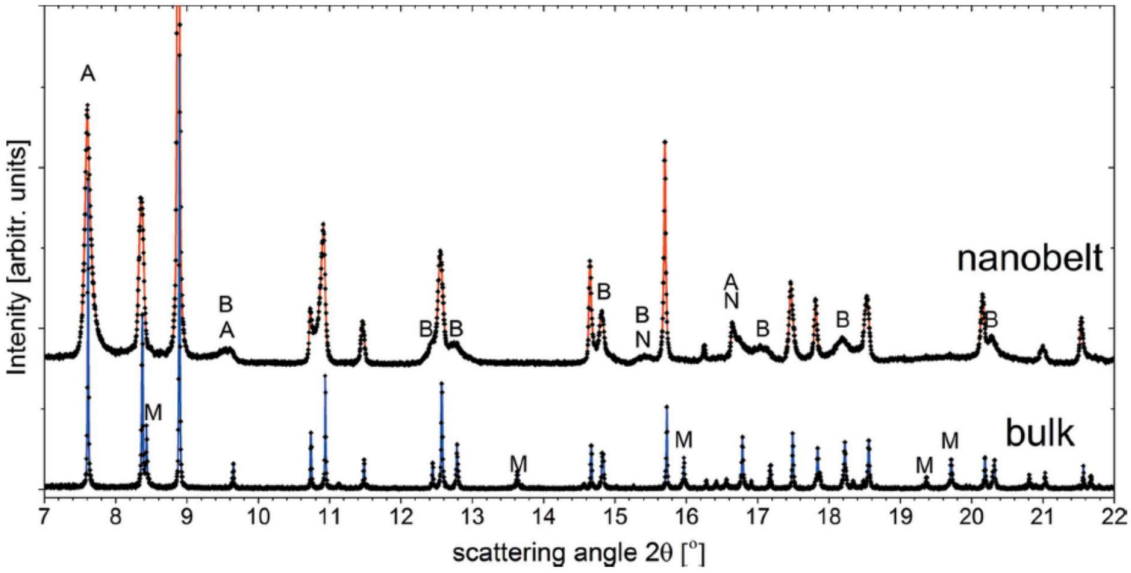

Figure 10 Synchrotron radiation based powder diffraction pattern measured on MoO_3 nanobelt (top) and bulk (bottom) samples; wavelength 0.50566 Å. Significant differences between the two patterns are marked: asymmetric peak shape (marked with A), significant peak anisotropic broadening (B),of the reflections was not observed for bulk material (N) and those were present only for the bulk sample (M). (Figure taken from paper **H5**).

described in **H1**. Based on this, it was possible to determine the structure of cobalt nanoparticles for different areas of the sample. Similarly, to the work presented in paper **H1**, it was necessary to assume that the material is a physical mixture of several (two) separate phases. It is important to note here that the analysis of diffraction data from the tomographic experiment must incorporate the multiple components present in the beam during the experiment and also the limited angular range of the measured diffraction patterns. Figure 9 shows the fitting result of the two-phase structural model of cobalt nanoparticles. The broadening of the diffraction peak around the scattering angle of 29° is clearly visible for the intergrowth phase (green line).

It was only because of advanced analysis of powder diffraction tomography experiment data that we were able to publish the work **H2** in the high-ranked journal *Science Advances*. This was possible due to the fact that I have taken into account that the structure of cobalt nanoparticles was disordered while performing the analysis. Otherwise, it would not be possible to correctly determine what crystalline phases arose as a result of chemical modification of the cobalt nanoparticles doped with TiO_2. The calculations I made were crucial for the quality of the paper.

The second nanomaterial, which required the use of the analysis method dedicated to partially disordered materials, was γ-MoO_3. This material, both in the bulk form, as well as nanosized

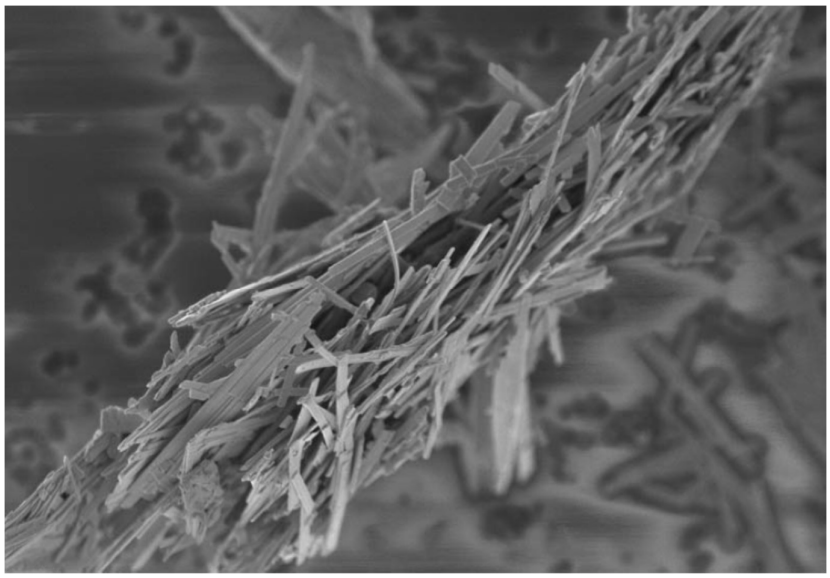

Figure 11 Scanning Electron Microscopy image of MoO_3 nanobelts (Figure taken from paper **H5**).

"nanobelts", exhibited interesting electrochemical properties [16, 17]. It is a potential candidate for cathode material in lithium-ion batteries [18]. The charge capacity measurements upon cycling (sequential charging and discharging) showed significant differences between the two forms of MoO_3. A battery whose cathode was made of MoO_3 nanoparticles, showed almost twice as long life and also almost doubled the maximum capacity as a standard battery. During battery cycling, lithium ions were repeatedly intercalated into the cathode. This resulted in different consequences for the cathode material [19, 20, 21], such as possible disorder in the structure, the transformation of the material into an amorphous form, the disintegration of crystallites or new compound formation. The essence of paper **H5** was the discovery of the causes of such large difference in chemical properties.

The measurements of synchrotron radiation-based powder diffraction for two forms of MoO_3 have revealed significant differences in the measured diffraction patterns. Figure 10 shows the comparison of the measured powder diffraction patterns for the two forms of MoO_3: bulk and nanoparticles (nanobelts). The positions of the measured diffraction maxima were identical and the corresponding peaks had similar intensities. However, the diffractograms differed significantly. The first significant difference was the substantial widening of the diffraction peaks for the nanomaterial. This was an expected effect, since the width of Bragg peaks are inversely proportional to the size of the crystallites in the material. However, it can be observed, that this broadening has an anisotropic character due to the significantly anisotropic shape of the nanomaterial crystallites. We performed scanning electron microscopy (SEM) measurements to confirm that, in fact, MoO_3 nanoparticles had the shape of cuboids, except

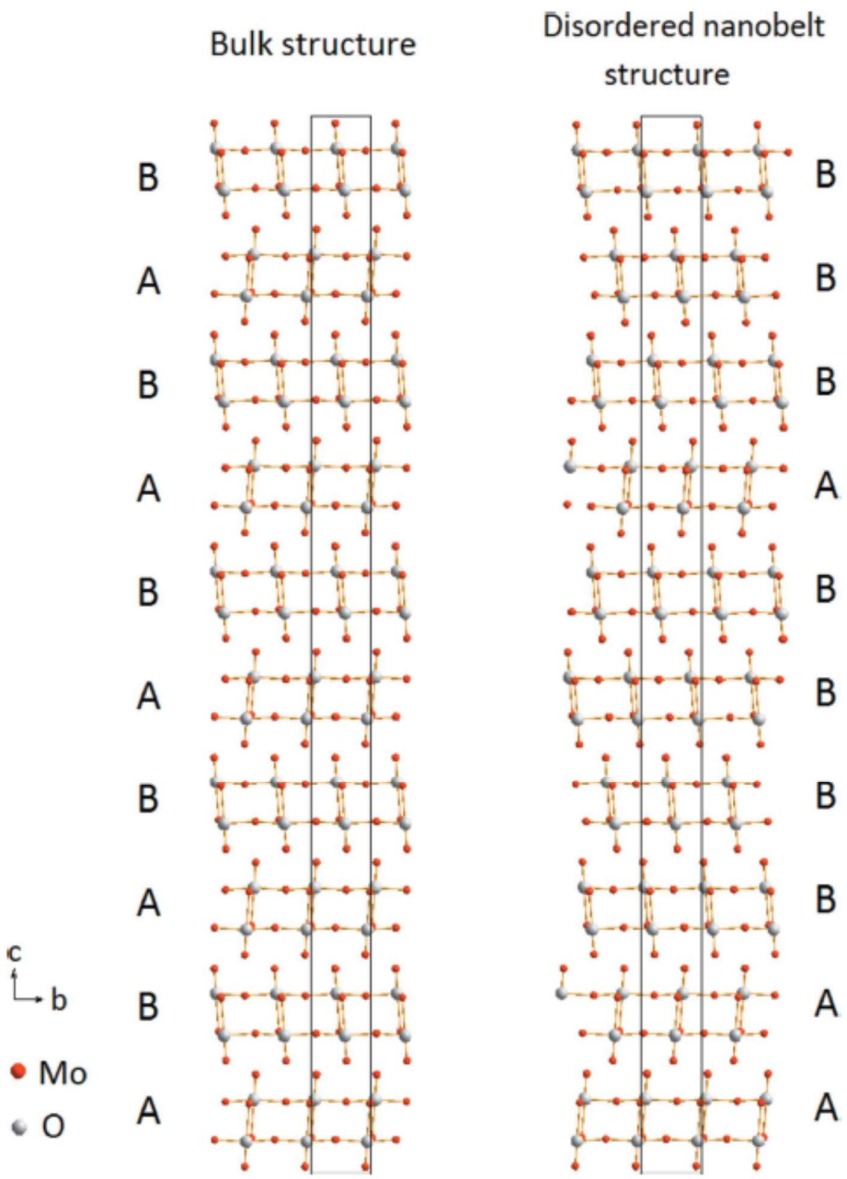

Figure 12 Crystal structure of MoO_3 (projection along [100]) in terms of stacked layers (10 layers = 5 unit cells). Left panel shows bulk α-MoO_3 (10 layers ordered in ABAB. . . sequence). The right panel presents an example of a stacking fault structure of nanobelt γ-MoO_3 (AABBBBABB... sequence with astacking fault probability A followed by B of 0.5) (Figure taken from paper **H5**).

that size in one direction was much larger than the other two (Figure 11). Even considering the belt-like anisotropic shape of crystallites it was not possible to describe the diffractogram of MoO_3 nanoparticles properly. The reason for the anisotropic broadening of Bragg maxima (marked as B) must therefore be of a different origin. The diffraction pattern also contained additional diffraction maxima (marked as N) and the shape of some of maxima were significantly asymmetrical (marked as A). Some of the Bragg peaks were also missing in the

powder pattern for the nanobelt MoO_3 sample (marked as M). This led to the conclusion that the structure of the two materials, despite many similarities, must be substantially different.

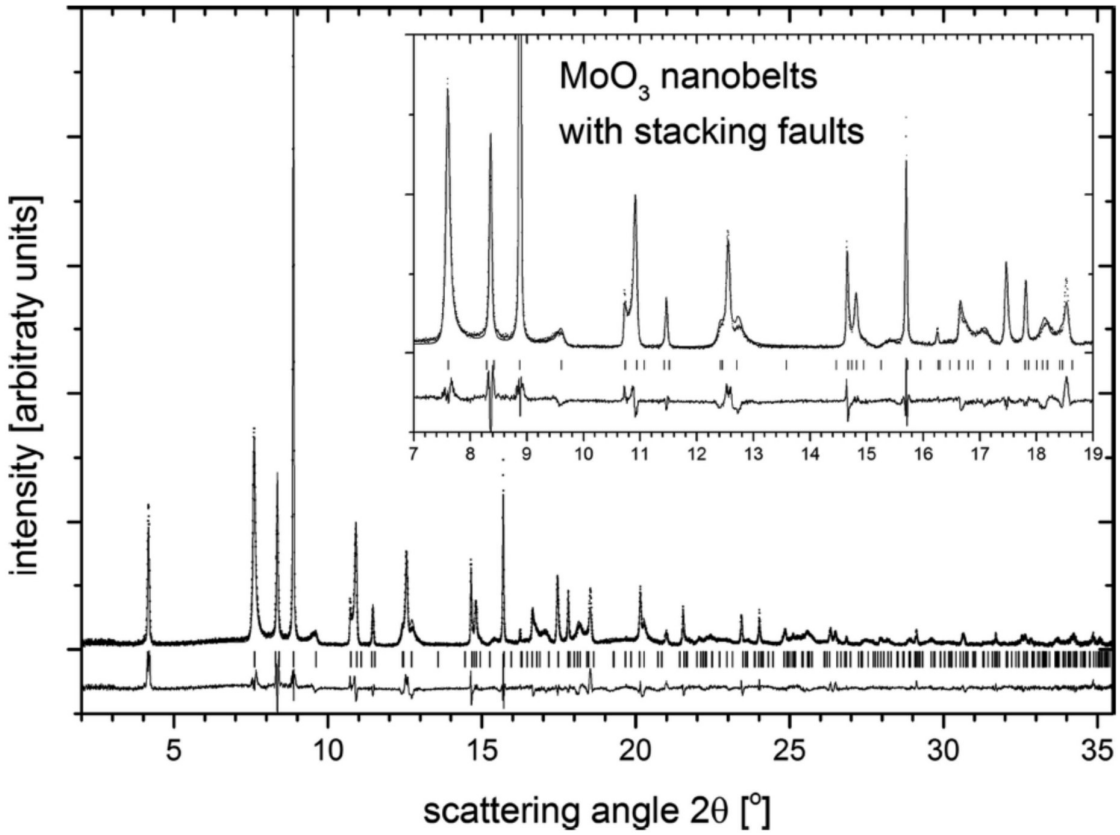

Figure 13 Synchrotron radiation based powder diffraction pattern for γ -MoO_3 nanobelts; wavelength 0.50566 Å. The experimental data and calculated profiles (calculated from the stacking fault model using the Discus package) are shown by points and a solid line respectively. Bragg positions (calculated for bulk α -MoO_3) are shown as bars. The difference curve is plotted below the fit (Figure taken from paper **H5**).

A closer look at the structure of bulk MoO_3 (Figure 12 left), allows us to recognise that the structure can be described in terms of altering layers. There are two different layers that can be distinguished and the second layer is a mirror image of the first one. The latter layer is also shifted in the *y* direction. The simulations performed by myself allowed the development of a structural model for MoO_3 nanoparticles. The three-dimensional structure is built in such a way that the two layers are randomly stacked on top of each other with a probability equal to 50%. An example of such a structure (random stacking) is shown in Figure 12 (right). The conclusion that MoO_3 nanobelts consist of randomly stacked layers enables us to explain all the characteristic features of the measured diffraction pattern (Figure 13). The disordered structure of MoO_3 nanobelts have been confirmed by transmission electron microscopy (TEM) (Figure 14). The TEM images in diffraction mode clearly show that the intensity along one direction

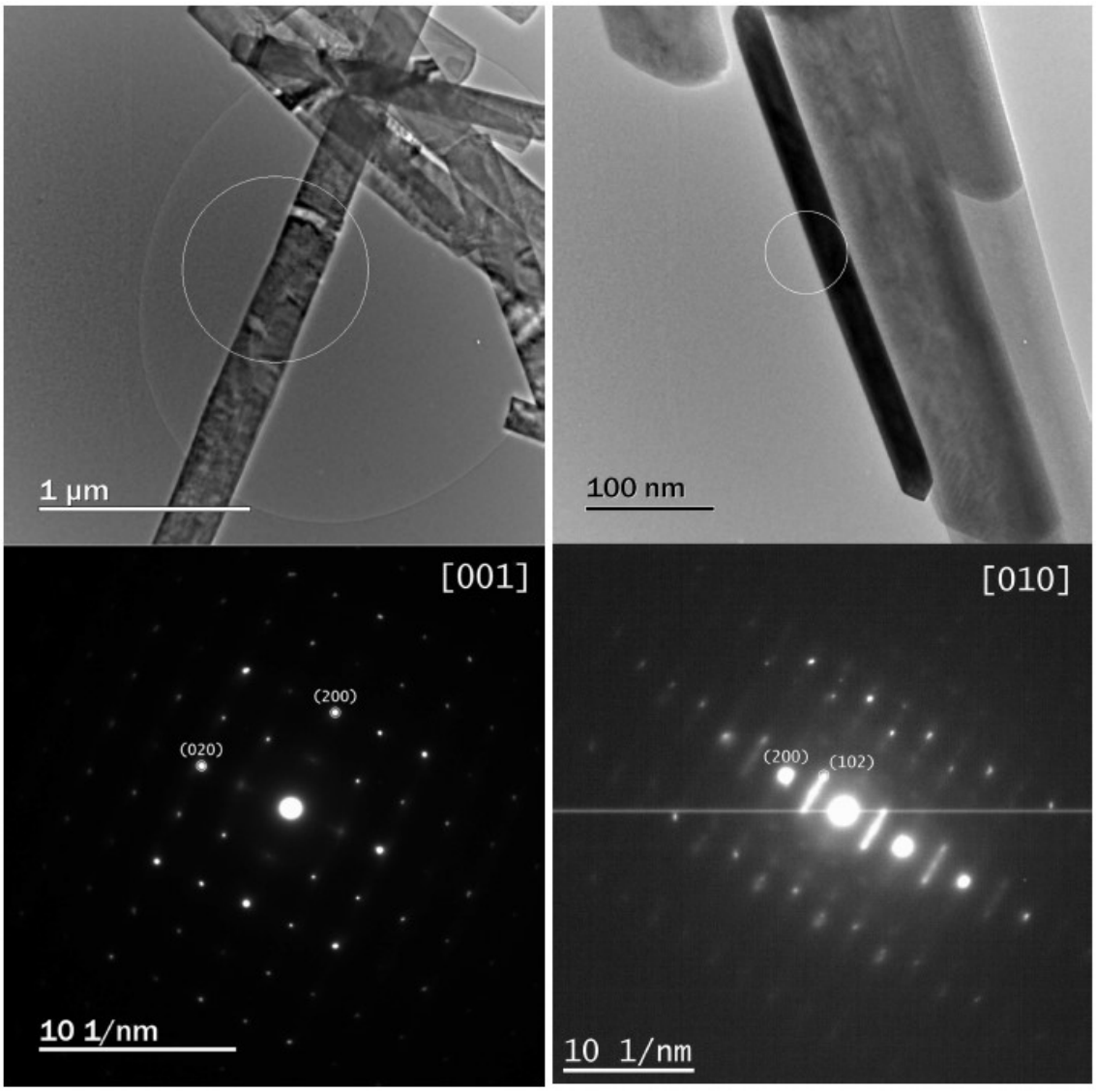

Figure 14 Transmission electron microscopy image of γ-MoO_3 nanobelts (top) oriented horizontally and vertically. The circle shows the area used for selected area electron difftacton SAED for the zone axis [001] and [010] (bottom). Bright diffraction spots in [001] plane are clearly observed (bottom, left). Intense diffuse scattering lines are observed along [001] (bottom, right). (Figure taken from paper **H5**).

has the form of intense lines, whereas in the other two directions only sharp spots are visible. The results obtained allowed the structure of γ-MoO_3 to be identified as a separate polymorph of MoO_3, as described in paper **H5**.

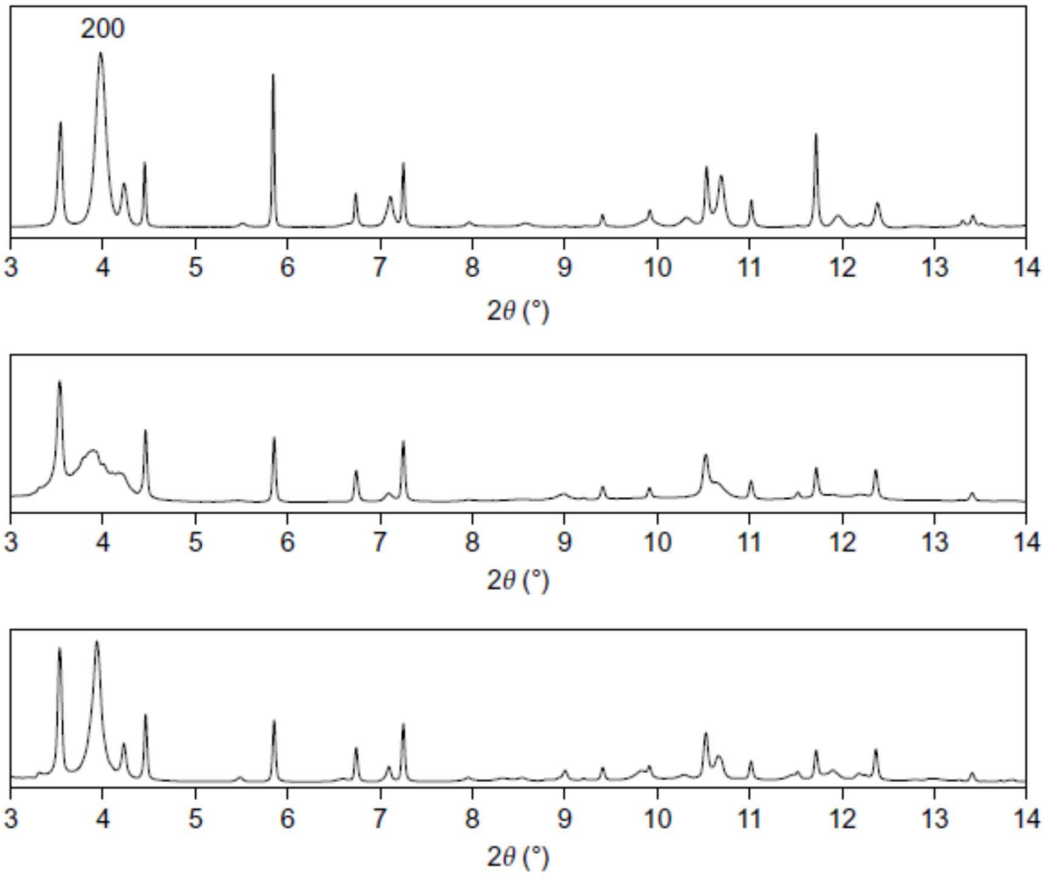

Figure 15 Comparion of three diffraction patterns: experimental data (top) and two calcualted based of different structural models – without and with interlayer distance conserved (middle and bottom) (Figure taken from the paper **H3**).

The second group of layered materials which show a high probability of faults in the arrangement of the crystalline layers are the zeolites. They show many potential applications, *e.g.* molecular sieves or catalysts [22]. This is an extremely rich family of materials mainly comprised of light elements such as Al, Si, O and P. Currently, the database of crystalline zeolite structures contains more than 230 items [23]. The crystal structure of zeolites can be represented in many ways. One such representation uses secondary building units containing up to several atoms. Those units can be joined together in a periodic manner in many ways, thus creating crystals [24]. The same units can be present in many different zeolite structures. Another way to represent the zeolite structure is to represent them in terms of layers. These layers can then be organized into a three-dimensional structure in multiple ways creating a periodic structure. In addition to three dimensional ordered structures, it is possible to obtain a

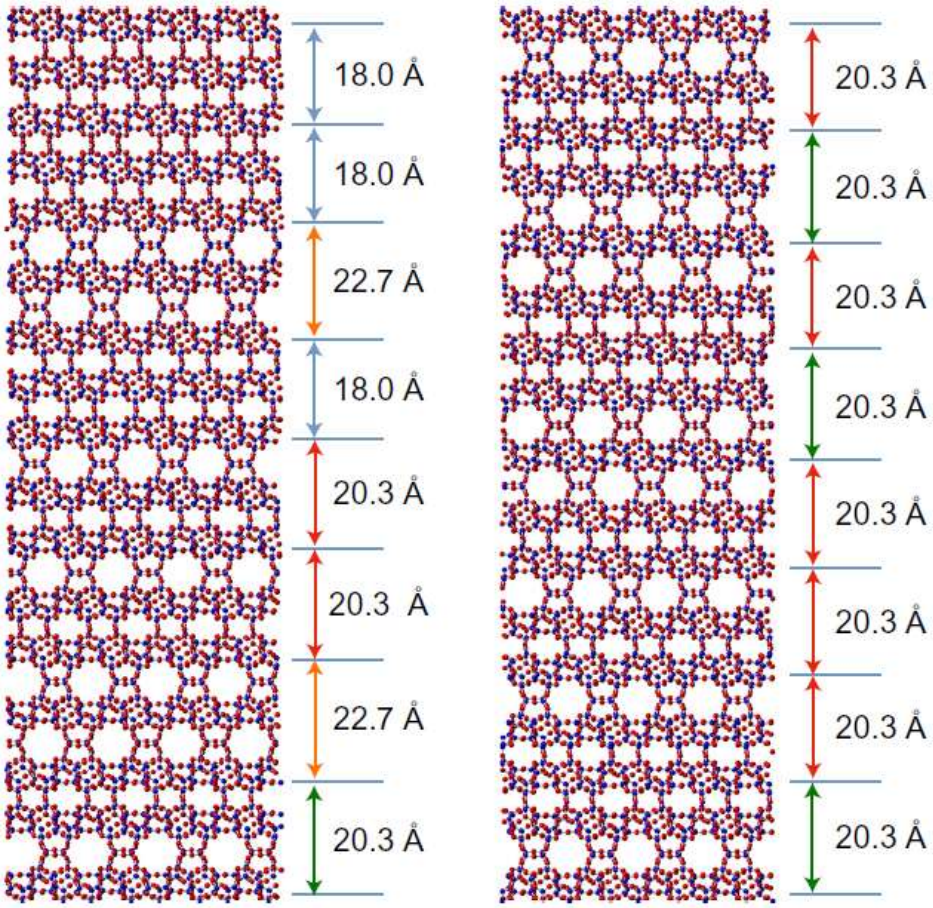

Figure 16 Two structural models of ICP-6 zeolite: random stacking of layers (with different interlayer distances) and such that the interlayer distance is conserved (allowing different layer orientation) (Figure taken from paper **H3**).

partially disordered structure. This can be also regarded as a co-existence of two zeolites within a single crystal [25]. Such crystals can also be called *intergrowth* structures, although strictly speaking the symmetry in one of the directions is not conserved.

A practical application of the modelling performed for a partially disordered zeolite structures was to describe the mechanism *assembly-disassembly-organization-reassembly* (ADOR) [26, 27, 28] for ICP-6 zeolite. This is a synthetic method for inorganic materials (including zeolites), consisting of 4 steps: *assembly* (preparation of the starting zeolite material), *disassembly* (partial degradation of the starting material, by removing selected subunits), *organization* (spatial reorganization of the crystalline units or layers) and *reassembly* (merging units/layers into a new structure). This process was described for zeolite ICP-6 in the paper **H3**. A precise description of this process would not be possible without the accurate crystal structure models at each of these stages, including possible faults in the order of layers. In the case of the IPC-

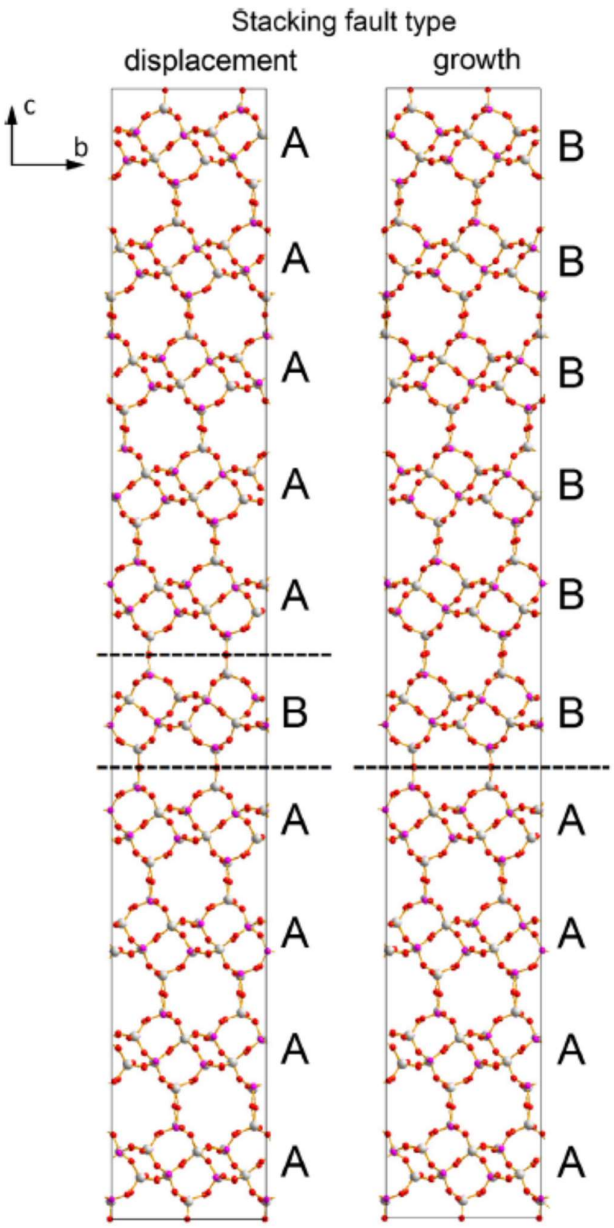

Figure 17 Crystal structure of faulted SAPO-18/34 family members. The left panel shows a *Displacement* type stacking fault. Two dashed lines indicate an introduced B-type layer which causes a stacking fault. The right panel shows a Growth type stacking fault. The dashed line indicates a change in the direction of crystal growth - the stacking fault. (Figure taken from paper **H7**).

6 zeolite, not only interlayer distances and layer orientations were an important parameter, but also the presence of additional sublayers (linkers) connecting the crystalline layers with each

other. Finally, it is the only correct description of the layered zeolite structure which gives a full picture of the structure at each stage of the ADOR.

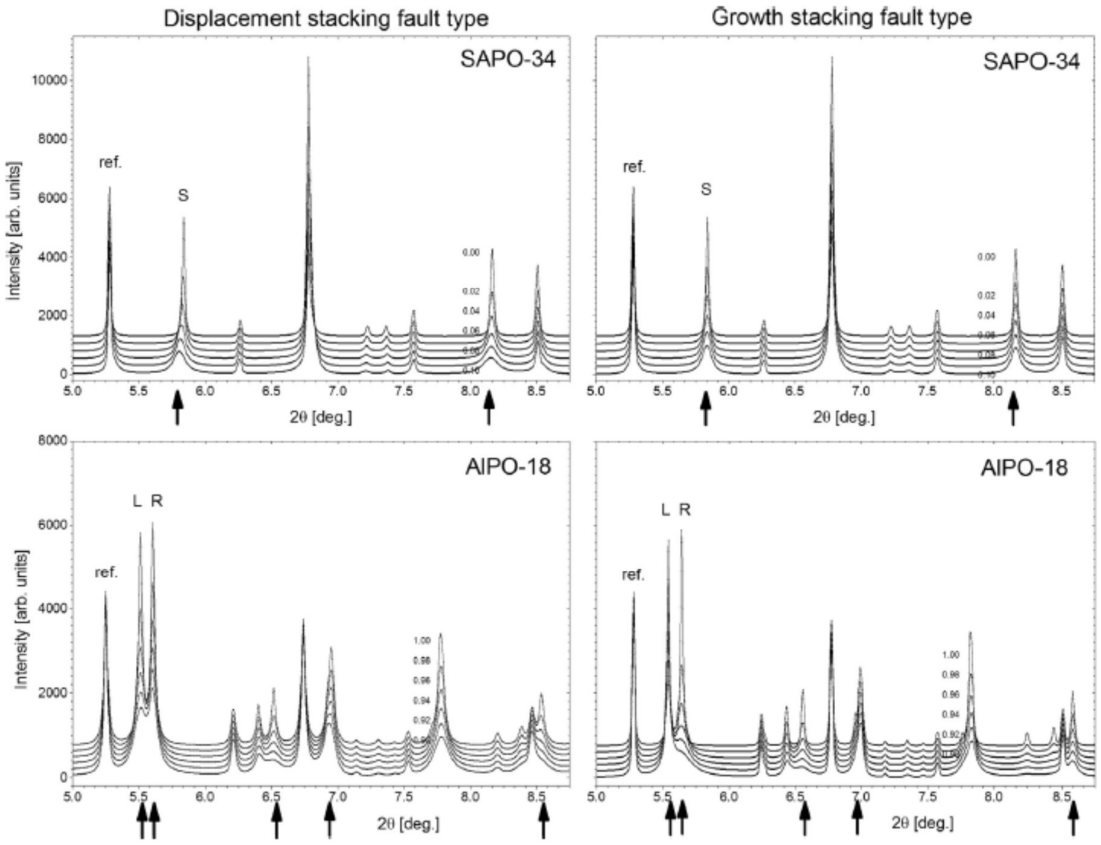

Figure 18 Series of calculated SR powder diffraction patterns of the SAPO-18/34 intergrowth family for low stacking fault probabilities. The top panels show patterns calculated for low probabilities based on SAPO-34. Two bottom patterns show patterns based on AlPO-18. The left and right panels show patterns calculated for *Displacement* and *Growth* stacking fault type structures, respectively. Arrows indicate diffraction maxima are strongly affected by stacking faults (Figure taken from paper **H7**).

Figure 15 presents the comparison of the measured diffraction pattern (top) and two simulated diffraction patterns, for two different structural models (middle and bottom). The first one is when three different layers are connected in a random way (middle). The second, when the constant interlayer distance is conserved (allowing also stacking faults resulting from mirroring of the layer) (bottom). The two model structures are shown on Figure 13.

A detailed investigation of the ADOR mechanism in the case of zeolites family member led to their publication in the high-ranked journal *Nature Chemistry*. My contribution to the publication was the calculation of powder diffraction patterns for different models of disordered crystal structure (described above), which allowed to identify the ADOR steps and describe the process in detail.

The second example the zeolites family is SAPO-18/34, the coexistence in one structure of the SAPO-18 and SAPO-34 in one crystal. This material is used as a catalyst in the methanol-to-olefin process (MTO) [29]. It is a very promising material due to the high selectivity of its reaction products and the high concentration and strength of the catalytically active sites [30]. Both the SAPO-18 and the SAPO-34 structures are built of the same secondary building units, spatially oriented in different ways. Alternatively, both structures can also be expressed in terms of identical layers arranged in different sequences (sequence AAAA ... corresponds to SAPO-34, while ABAB ... to SAPO-18) or to mix the two structures into an *intergrowth* structure. A correlation between the probability of staking faults and the efficiency of the MTO process was also observed [31]. In my papers **H7** and **H6** the study of this zeolite family was described.

In the work **H7** I described in detail the structural details for compounds from the SAPO-18/34 zeolite family. The structure of both SAPO-18 and SAPO-34 consists of two identical layers A and B (layer B is a mirror image an A layer). The structure of SAPO-18 is created as a sequence of ABAB ... layers stacked, while SAPO-34 as AAAA ... or BBBB ... staking. Each deviation from those layer sequences create defects (if only the probability of those faults is relatively low, one can just say about the structure with defects). However, for higher probability of stacking faults one should model the crystal as the *intergrowth structure*. Other works have also demonstrated a coexistence of both SAPO-18 and SAPO-34 structures within the same crystal. In paper **H7** I described two possible models for defect formation of staking the crystalline layers, named *Displacement* and *Growth*. Figure 17 shows the two corresponding defect models. Finally, even when there is a small probability for defects to occur, powder diffraction is a very sensitive experimental method to detect them.

Figure 18 shows simulated diffraction patterns for SAPO-18 structures (also referred to as AlPO-18) and SAPO-34 for two different stacking fault types and probabilities of stacking faults from 0 to 10%. Arrows indicate the diffraction peaks that strongly depend on the probability of stacking faults. Their intensity and width changes dramatically. It is also clearly visible that the intensities of those diffraction peaks change in different ways depending on the type of stacking faults used: *Displacement* or *Growth*. Those dependencies can be used as a simple probe of the probability of stacking faults, as described in detail in paper **H7**. This is a prominent result. That the detailed analysis of the measured diffraction patterns require a full refinement of the structure using the Discus program, which can also be replaced by a simple analysis of selected diffraction peak widths should also be noted. The alternative method also gives very precise results. This method may, for example, be used to describe disordered crystal structures based on powder diffraction patterns of patented compounds [31, 32, 33].

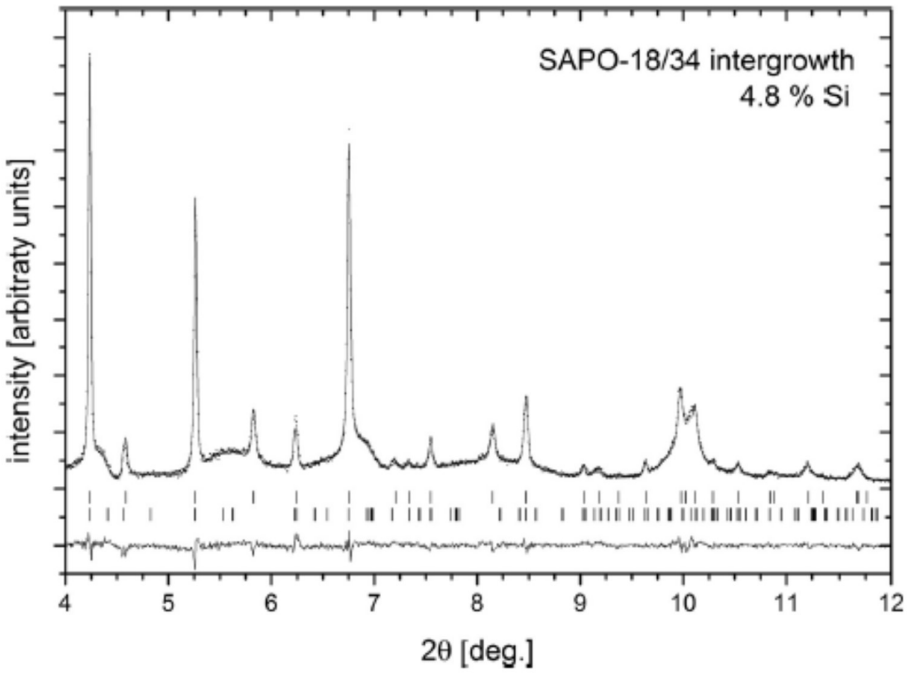

Figure 18 Powder diffraction pattern measured for SAPO-18/34 doped with 4.8 % Si, with refinement based on the stacking faults model of the *Displacement* type (Figure taken from paper **H7**).

Figure 18 shows an example of the crystal structure refinement for SAPO-18/34 with 4.8% Si content. One can see both narrow Bragg peaks as well as wide often asymmetrical maxima caused by the disordered nature of this structure. It was also possible to estimate the phase composition of the material as a mixture of two crystalline phases with different levels of stacking faults.

Based on the performed simulations and calculations (similar to that shown in Figure 19) for the SAPO-18/34 family members doped with Si in the range from 0 to 7.5%, the phase diagram was determined as presented in **H6** (Figure 20). It shows that SAPO-18/34 materials doped with Si are composed as mixtures of three crystalline phases with different probabilities of stacking faluts. These three phases were assigned to other crystal growth mechanisms (symbolically represented in the form of drawings on a phase diagram), which was observed by means of atomic force microscopy (AFM).

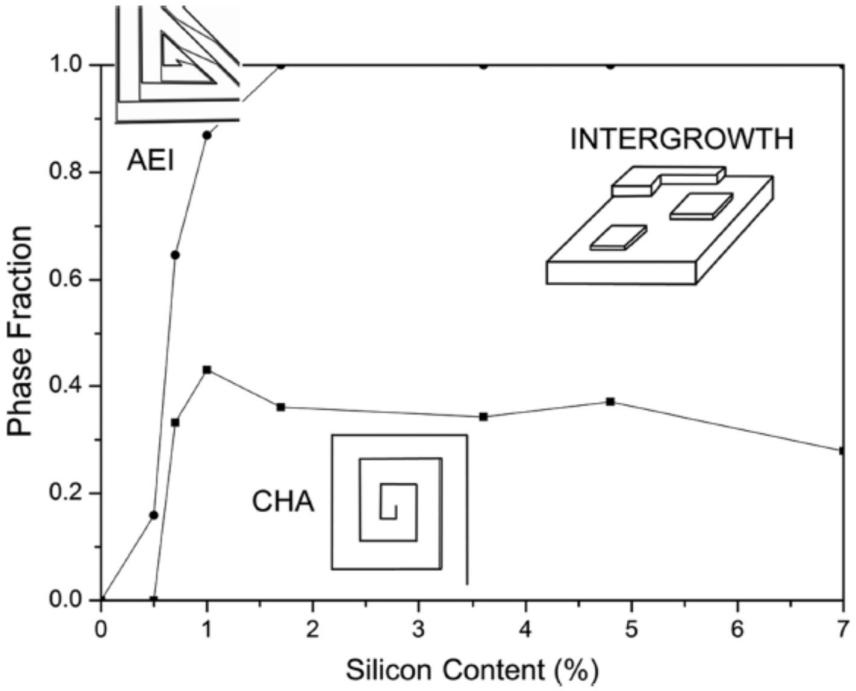

Figure 20 Phase diagram of SAPO-18/34 as a funciton of Si doping. Three crystalling phases with different levels of disoder are present (Figure taken from paper **H6**).

The correctness of the model used with multiple crystalline phases which describes the measured diffraction patterns in detail, has been verified by measurements of nuclear magnetic resonance (NMR). Based on the results from NMR experiments for phosphorus and carbon, the probability of the P and C atoms being located at the local environment typical for SAPO-34 was established. In other words, it was determined how often the successive layers create subunits characteristic of SAPO-34. These results were compared to those obtained from powder diffraction experiments. These results are extremely consistent, as shown in

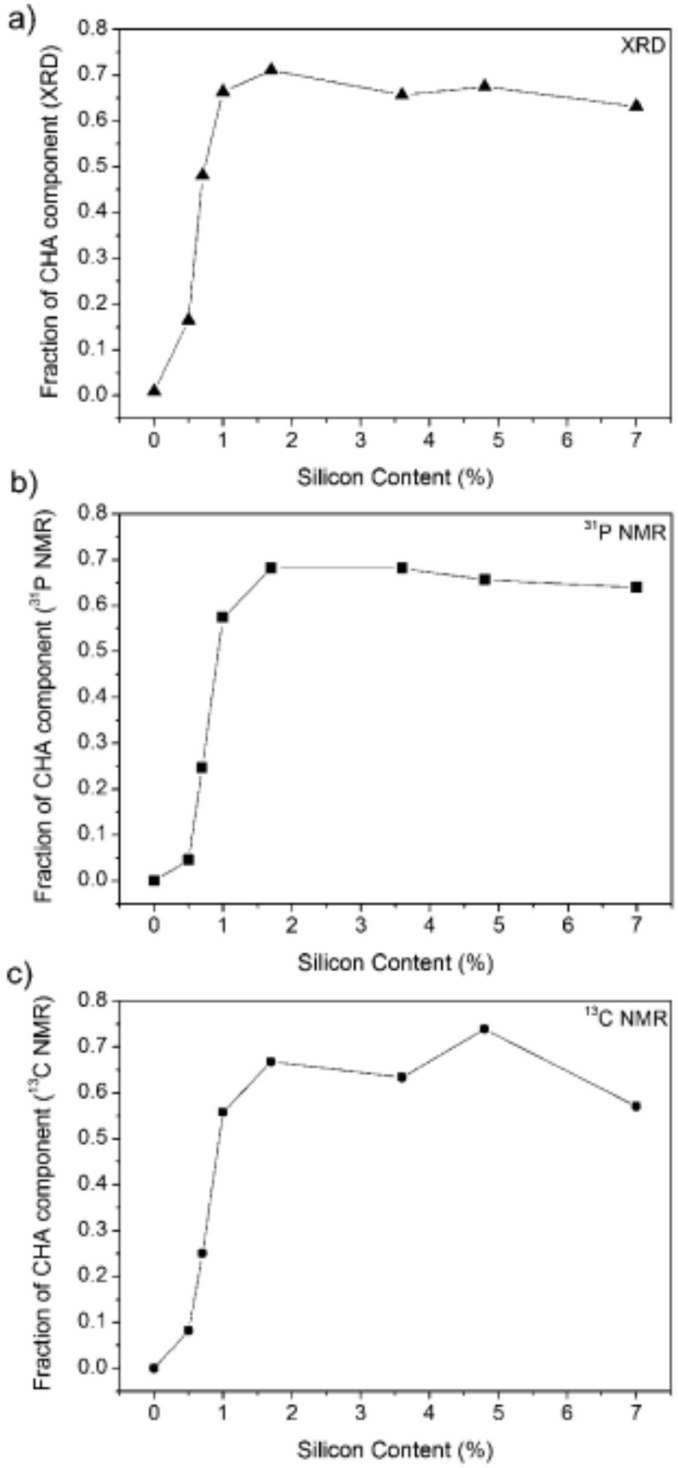

Figure 21 Estimated amount of SAPO-34 interlayer connections as a function of Si doping. The values are taken from synchrotron radiation data (panel a) and NMR measurement (panel b and c) (Figure taken from **H6**).

Figure 21. It can therefore be assumed that the multiphase model for SAPO-18/34 system is close to the real structure of the materials used.

The last part of the work presented here, is my study of modelling of disordered structures of *Layered Double Hydroxides (LDH)*. These materials have multiple applications: catalysis, sorption and gas separation, medicine, as pigments, as thermal barriers and energy generators [34, 35, 36, 37, 38, 39, 40]. The LDHs are built of flat, positively charged layers with crystalline structure, separated from each other by negative anions. There is a huge diversity of materials within this group (different elements forming crystalline layers and a variety of anions placed in between the layers). The anions in the interlayer gallery can have very different sizes, even up to 15 Å. It is relatively easy to change structural properties of the material by placing different anions in between the layers, or by changing their orientation. Because the crystalline layers are separated by a spatial distance from each other, they interact with each other only electrostatically and so they remain only weakly bound together. This is the main reason why various kinds of disorder are possible. The space between the crystalline layers can also be filled up with water molecules.

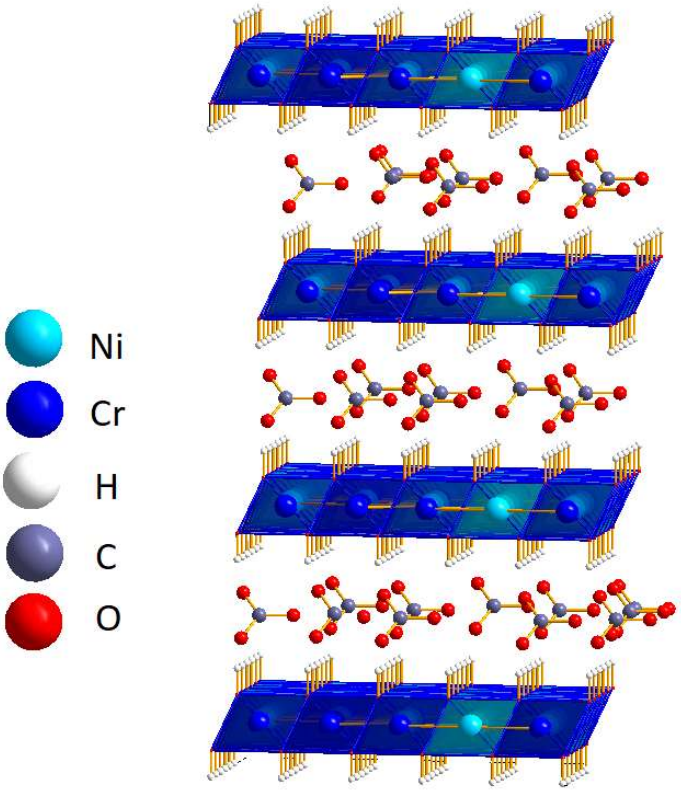

Figure 22 Schematic representation of *Layered Double Hydroxides* (LDH) crystal structure.

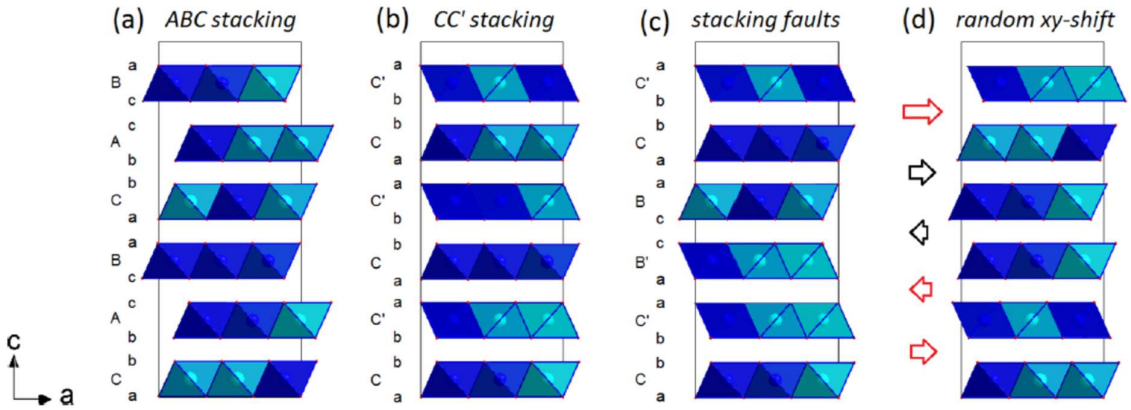

Figure 23 Schematic illustration of (a) perfect order of ABC stacking, (b) perfect order of CC' stacking, (c) stacking fault structure, and (d) random xy-shift layered structure. For random xy-shift black and red arrows present interlayer shifts. The colors denote the change of the layer type: red (change from "left-hand side" to "right-hand side" or the opposite) and black (no change) (Figure taken from **H4**).

Figure 22 schematically shows the structure of LDHs without possible disorder in the layer stacking. In **H4** I presented the impact of various aspects of structural disorder on the simulated powder diffraction patterns. I have also analysed the influence of different arrangement of interlayer space filling on simulated diffraction patterns.

The first type of disorder is the intergrowth of two possible structures, a sequence of successive layers described as ABC and CC' stacking called *stacking faults*. The parameter describing

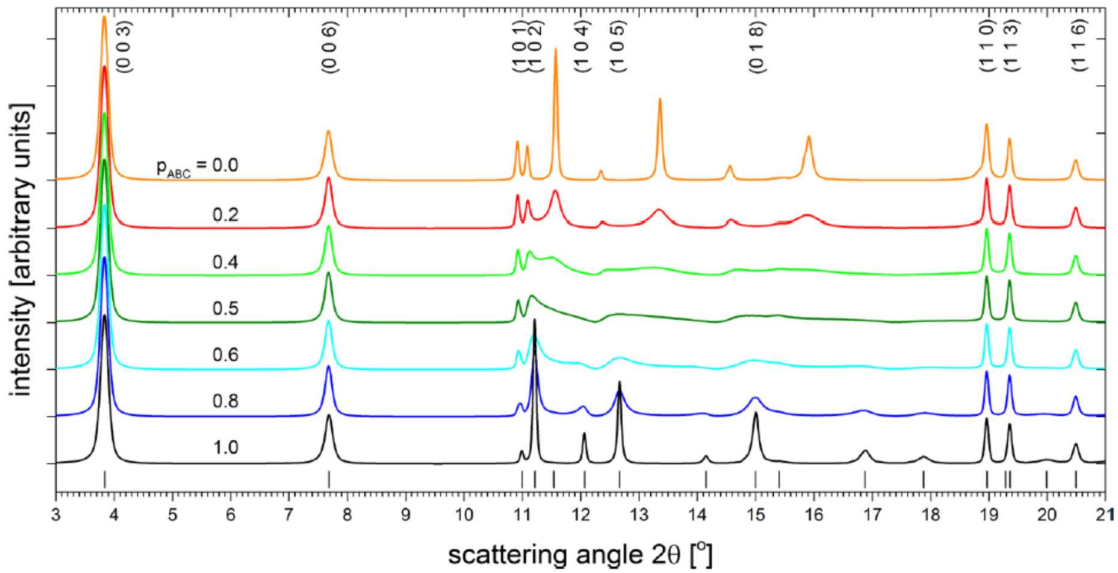

Figure 24 Series of X-Ray powder difftaction patterns of *Layered Dobule Hydroxides* with probability of stacking faults p_{ABC} from 0.0 to 1.0. The (hkl) indices and Bragg reflection positions correspond to the hexagonal unit cell of the ideal ABC... stacked structure. The probability of stacking faults p_{ABC} = 0.5 describes fully random stacking of LDH layers of ABC or CC′ type. (Figure taken from paper **H4**).

this kind of disorder will be p_{ABC} which is the probability that subsequent layers form a structure of the ABC type.

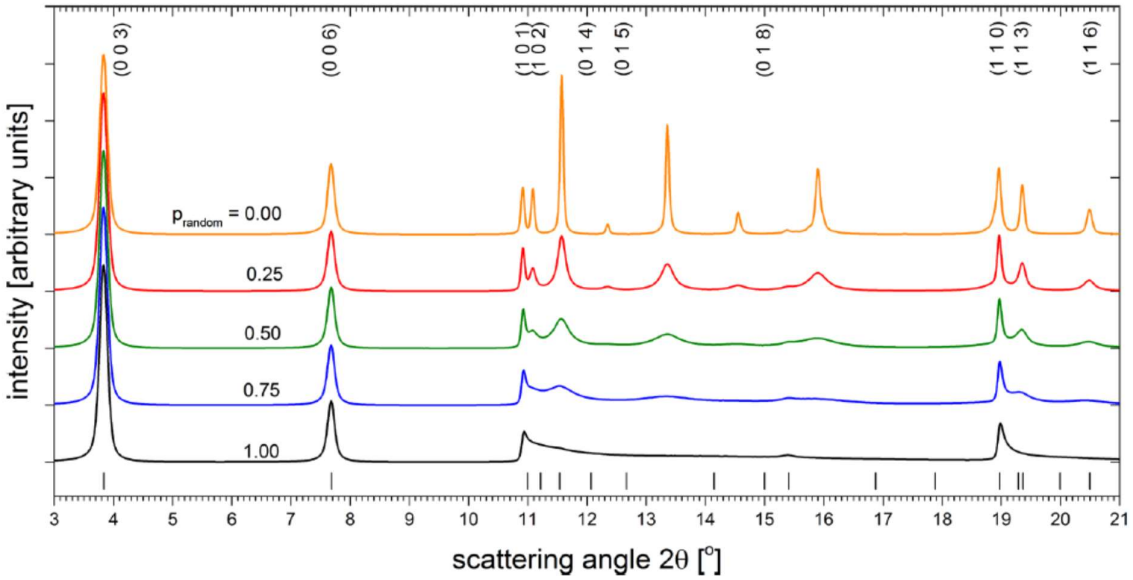

Figure 25 Series of X-Ray powder difftaction patterns of *Layered Dobule Hydroxides* with probability of random xy-shift p_{random} from 0.0 to 1.0. The (hkl) indices and Bragg reflection positions correspond (for purpose of comparison) to the hexagonal unit cell of an ideal ABC... tacked structure. The probability of xy-shift p_{random} = 1.0 describes fully disordered structure of LDH layers with no xy-interlayer correlations; p_{random} = 0.0 corresponds to the CC′ stacking type. p_{ABC} = 0.0 in all simulations. (Figure taken from paper **H4**).

The second type of disorder considered is the structure in which the two consecutive layers are shifted by a random vector in the plane of the layer (plane xy) relative to each other. In this case, the interlayer distance between the layers is conserved, while there is no such conservation in the xy plane.

Figure 23 shows the structures described above. In the case of ABC and CC' structures, the layers are arranged in a periodic way, and so the calculated diffraction patterns will consist of characteristic narrow Bragg peaks. In the case of structures with stacking faults or with no xy interlayer correlation, some of the diffraction peaks are asymmetrical, with Warren type peak shape [41].

Figure 24 shows a series of powder diffraction patterns calculated for structures with a different probability of stacking faults described by p_{ABC} parameter (the probability that the layers are stacked in the ABC sequence). The ABC structure type corresponds to p_{ABC} = 1.0 and CC' to p_{ABC} = 0.0, while the fully random structure has p_{ABC} = 0.5. For a completely random structure one can see the characteristic triangular shapes of the selected diffraction peaks. On the other hand, the (00L) reflections remain unchanged, regardless of the sequence of layers.

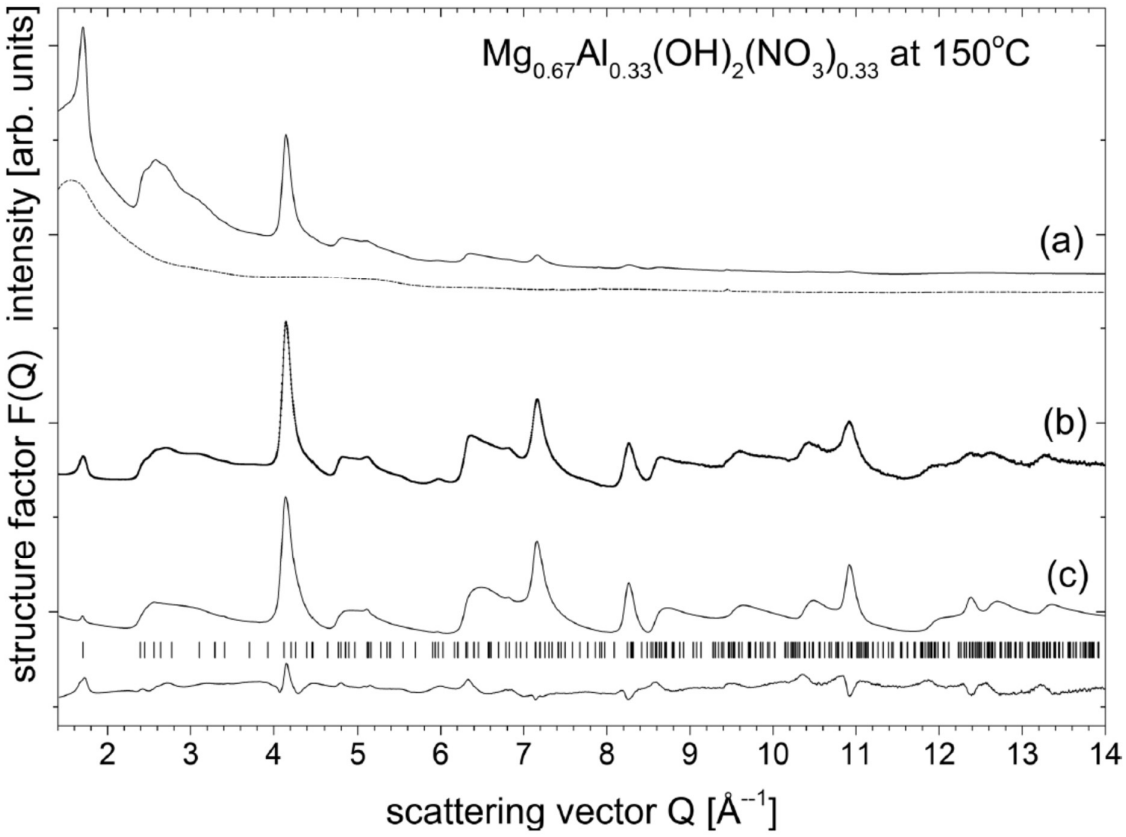

Rysunek 2 Powder X-Ray diffraction pattern for $Mg_{0.67}Al_{0.33}(OH)_2(NO_3)_{0.33}$ heat treated at 150 °C (panel a, solid line) together with the background subtracted (dashed line). Panels b and c show measured and refined structure factor F(Q). Below are shown the Bragg peak positions and the difference curve. All patterns are shown in scattering vector Q scale. See text for the structure description details (Figure taken from paper **H4**).

The second example of a partially disordered structure is the structure when the layers are randomly shifted in the plane of layers (xy plane). Figure 25 shows a series of diffraction patterns obtained for structures with different probability of a random xy shift as denoted by p_{random} . The three-dimensional periodic structure corresponds to $p_{random} = 0.0$, while if $p_{random} = 1.0$, all the crystalline layers will have a random shift relative to the neighbouring layer. In this case, apart from unchanged diffraction peaks of (00L) type, one can see only very broad, asymmetrical maxima with a very elongated shape towards the larger diffraction angles.

In **H4** I also described a number of other parameters which can be investigated by powder diffraction measurements which significantly change the LDH structure. Those are: the water content in the interlayer gallery, the orientation of the anions in the space in between the layers, the number of layers that form a crystalline slab and the distribution of interlayer distances. The calculated diffraction patterns presented in **H4** allows recognition of the individual parameter influences on the simulated powder diffraction pattern and thus determination of the type of disorder that is present in the actual sample. Quite often, the authors of other works

limit themselves to descriptions of the structure as having a "structure with stacking faults", but they are not able to describe this phenomena in detail [42, 43, 44, 45]. Therefore, the presented library of calculated powder diffraction patterns can be very useful.

As a final part **H4** I demonstrated the application of a new method of the analysis of diffraction data for partially disordered structures, as shown by the example of LDH type compounds. A common problem caused by difficulties in the obtaining large crystals, combined with a significant level of disorder, is the relatively small number of recognisable diffraction peaks (in a standard powder diffraction experiment using synchrotron radiation). This makes it difficult to determine the parameters of the material precisely. Figure 26 (top) shows the measured powder diffraction pattern for LDH $Mg_{0.67}Al_{0.33}(OH)_2(NO_3)_{0.33}$ at 150°C. There are only two distinctive diffraction maxima, as well as a series of small, poorly visible, asymmetrical peaks. Traditional analysis of these experimental data would not be possible. Therefore, I used the method of transforming the measured diffraction pattern (intensity as a function of the scattering vector Q) to the structure factor F (Q) by using the PDFGetX3 program [46] dedicated for data reduction to the pair distribution function (PDF) (the F(Q) which is shown in Figure 26 (middle). This transformation reveals a series of additional diffraction peaks with a characteristic, triangular shape. Thanks to the help of Prof. Reinhard Neder (University of Erlangen, Germany, the main author of the *Discus* program), who added some missing functionalities to *Discus* program, I was able to refine the structural parameters against the experimental data represented by the F(Q) function. The calculated structure factor F (Q) is shown in Figure 26 (bottom). Based on the calculations carried out, the $Mg_{0.67}Al_{0.33}(OH)_2(NO_3)_{0.33}$ structure was identified as an 88.9% fraction of two-dimensional crystalline layers that did not form any three-dimensional structure and 11.1% of the three-dimensional structure of the random xy-shift type disordered structure, with the probability of an xy-shift close to 1. This means that the new method enables the application of the powder diffraction technique for the analysis of two-dimensional objects as well.

Summary

The analysis of powder diffraction patterns applied to partially disordered materials, as presented in the first part of this summary, has not been widely known and used by the community in the determination of structures of this type of materials. In many cases the authors have limited themselves to the statement that the material may contain significant level of defects or stacking faults, but they were not able to take this fact into account during the analysis of the diffraction data. The method I presented was not directly developed by myself, but its application, development and usage is my original contribution to the development of research on partially disordered materials.

My most important achievement presented in this summary, is, as I believe, the development of nthe poorly known method of analysing materials where it is crucial to take into account the disorder in the crystal structure and its successful application to several disordered structures.

The application of this method, mentioned above, allowed the development of much more accurate crystal structure models of the materials studied. In the papers **H1**, **H4** and **H7**, the collections of simulated diffraction patterns are shown, which allows their use as a library for direct comparison with the experimental data and preliminary determination of the type of disorder. It also allows estimation of the probability of a particular disorder type to occur.

Within the publications **H6** and **H7**, I have presented the development of structural models and phase diagrams for SAPO-18/34 zeolite family members. These works became the starting point for the collaboration which resulted in the publication of **H3**, where we described a new mechanism for the synthesis of zeolites, unknown before this publication. The paper **H3** was published in the prestigious journal *Nature Chemistry*. The description of this mechanism would not be possible without the development of more accurate crystal structure models of these zeolites thatI have performed which takes into account their partly disordered nature.

In publications **H1** and **H5** I have demonstrated the application of disordered structural modelling to nanomaterials. In **H5** I discovered a new polymorphic form of the MoO_3 material, while the results of **H1** were the starting point for establishing a larger collaboration which resulted in the publication **H2**, which was published in the high-ranked journal *Science Advances*. The models of cobalt nanoparticles detailed therein were used to describe the X-ray tomography from experimental data of a sample similar to materials used in catalytic applications.

References

[1] [Online]. Available: http://reference.iucr.org/dictionary/Crystal.

[2] W. Friedrich, P. Knipping and M. Laue, "Interferenzerscheinungen bei Röntgenstrahlen," *Annalen der Physik,* vol. 346, pp. 971-988, 1913.

[3] W. L. B. W. H. Bragg, "The Reflection of X-rays by Crystals," *Proc. R. Soc. Lond. A,* 1913.

[4] T. Proffen and R. B. Neder, *Journal of Applied Crystallography,* vol. 30, pp. 171-175, 1997.

[5] E. Rytter and A. Holmen, "Deactivation and regeneration of commercial type fischer-tropsch co-catalystse - A mini-review," *Catalysts,* vol. 5, pp. 478-499, 2015.

[6] B. Morcos, P. Lecante, R. Morel, P.-H. Haumesser and C. C. Santini, “Magnetic, Structural, and Chemical Properties of Cobalt Nanoparticles Synthesized in Ionic Liquids,” *Langmuir,* vol. 34, pp. 7086-7095, 2018.

[7] A. A. Mirzaei, M. Arsalanfar, H. R. Bozorgzadeh and A. Samimi, “A review of Fischer-Tropsch synthesis on the cobalt based catalysts,” *Physical Chemistry Research,* pp. 179-201, 2014.

[8] H. Jahangiri, J. Bennett, P. Mahjoubi, K. Wilson and S. Gu, “A review of advanced catalyst development for Fischer-Tropsch synthesis of hydrocarbons from biomass derived syn-gas,” *Catalysis Science and Technology,* vol. 4, pp. 2210-2229, 2014.

[9] N. E. Tsakoumis, E. Patanou, S. Lögdberg, R. E. Johnsen, R. Myrstad, W. Beek, E. Rytter and E. A. Blekkan, “Structure–Performance Relationships on Co-Based Fischer–Tropsch Synthesis Catalysts: The More Defect-Free, the Better,” *ACS Catalysis,* vol. 9, pp. 511-520, 2019.

[10] A. T. Bell, “The Impact of Nanoscience on Heterogeneous Catalysis,” 2003. [Online]. Available: http://science.sciencemag.org/content/299/5613/1688.

[11] M. Mavrikakis, B. Hammer and J. K. Nørskov, “Effect of Strain on the Reactivity of Metal Surfaces,” *Phys. Rev. Lett.,* vol. 81, no. 13, pp. 2819-2822, 9 1998.

[12] J. K. Nørskov, F. Abild-Pedersen, F. Studt and T. Bligaard, “Density functional theory in surface chemistry and catalysis,” *Proceedings of the National Academy of Sciences,* vol. 108, pp. 937-943, 2011.

[13] A. L. Cabrera, N. D. Spencer, E. Kozak, P. W. Davies and G. A. Somorjai, "Improved instrumentation to carry out surface analysis and to monitor chemical surface reactions in situ on small area catalysts over a wide pressure range (10-8-105 Torr)," *Review of Scientific Instruments,* vol. 53, pp. 1888-1893, 1982.

[14] B. J. McIntyre, M. Salmeron and G. A. Somorjai, "A variable pressure/temperature scanning tunneling microscope for surface science and catalysis studies," *Review of Scientific Instruments,* vol. 64, pp. 687-691, 1993.

[15] G. K. Williamson and W. H. Hall, "X-ray line broadening from filed aluminium and wolfram," *Acta Metallurgica,* vol. 1, pp. 22-31, 1953.

[16] R. Nadimicherla, Y. Liu, K. Chen and W. Chen, "Electrochemical performance of new α-MoO3 nanobelt cathode materials for rechargeable Li-ion batteries," *Solid State Sciences,* vol. 34, pp. 43-48, 2014.

[17] B. Scrosati, "Challenge of portable power," *Nature,* vol. 373, pp. 557-558, 1995.

[18] A. Kraytsberg and Y. Ein-Eli, “Higher, Stronger, Better… A Review of 5 Volt Cathode Materials for Advanced Lithium-Ion Batteries,” *Advanced Energy Materials,* vol. 2, pp. 922-939, 2012.

[19] J. Lee, A. Urban, X. Li, D. Su, G. Hautier and G. Ceder, "Unlocking the potential of cation-disordered oxides for rechargeable lithium batteries," *Science,* vol. 343, pp. 519-522, 2014.

[20] J. Chen, "Recent progress in advanced materials for lithium ion batteries," *Materials,* vol. 6, pp. 156-183, 2013.

[21] C. Sun, R. Hui and J. Roller, "Cathode materials for solid oxide fuel cells: A review," *Journal of Solid State Electrochemistry,* vol. 14, pp. 1125-1144, 2010.

[22] S. C. Larsen, “Nanocrystalline Zeolites and Zeolite Structures: Synthesis, Characterization, and Applications,” *The Journal of Physical Chemistry C,* vol. 111, pp. 18464-18474, 2007.

[23] [Online]. Available: http://europe.iza-structure.org/IZA-SC/ftc_table.php.

[24] B. M. Weckhuysen and J. Yu, “Recent advances in zeolite chemistry and catalysis,” *Chem. Soc. Rev.,* vol. 44, no. 20, pp. 7022-7024, 2015.

[25] G. O. N. G. Li-Yuan SUN andYa-Fei ZHANG andYan-Jun, “Structural Features and Application of Micro-Microporous Composite Zeolites,” *Acta Physico-Chimica Sinica,* vol. 32, p. 1105, 2016.

[26] M. Mazur, P. S. Wheatley, M. Navarro, W. J. Roth, M. Položij, A. Mayoral, P. Eliášová, P. Nachtigall, J. Čejka and R. E. Morris, "Synthesis of 'unfeasible' zeolites," *Nature Chemistry,* vol. 8, pp. 58-62, 2016.

[27] P. Eliášová, M. Opanasenko, P. S. Wheatley, M. Shamzhy, M. Mazur, P. Nachtigall, W. J. Roth, R. E. Morris and J. Čejka, "The ADOR mechanism for the synthesis of new zeolites," *Chemical Society Reviews,* vol. 44, pp. 7177-7206, 2015.

[28] W. J. Roth, P. Nachtigall, R. E. Morris, P. S. Wheatley, V. R. Seymour, S. E. Ashbrook, P. Chlubná, L. Grajciar, M. Položij, A. Zukal, O. Shvets and J. Čejka, "A family of zeolites with controlled pore size prepared using a top-down method," *Nature Chemistry,* vol. 5, pp. 628-633, 2013.

[29] J. Q. Chen, A. Bozzano, B. Glover, T. Fuglerud and S. Kvisle, "Recent advancements in ethylene and propylene production using the UOP/Hydro MTO process," *Catalysis Today,* vol. 106, pp. 103-107, 2005.

[30] F. Bleken, M. Bjørgen, L. Palumbo, S. Bordiga, S. Svelle, K.-P. Lillerud and U. Olsbye, “The Effect of Acid Strength on the Conversion of Methanol to Olefins Over Acidic Microporous Catalysts with the CHA Topology,” *Topics in Catalysis,* vol. 52, pp. 218-228, 01 4 2009.

[31] M. Janssen, A. Verberckmoes, M. Mertens, A. Bons and W. Mortier, *ExxonMobile Chemical Europe Inc.,* vol. patent no. EP 1 365 992 B1 (2007), 2007.

[32] R. Wendlebo, D. E. Akporiaye, A. Anderson, M. I. Dahl, H. B. Mostad, T. Fuglerud and S. Kvisle, “Microporous crystalline silicoalumino-phosphate composition, catalytic material comprising said composition and use of these for production of olefins from methanol.,” *U.S. Patent 6,334,994,* 2012.

[33] M. M. Mertens, “Synthesis and use of aei structure-type molecular sieves.,” vol. WO 2009/117186, 2009.

[34] R. Yang, Y. Gao, J. Wang and Q. Wang, "Layered double hydroxide (LDH) derived catalysts for simultaneous catalytic removal of soot and NOx," *Dalton Transactions,* vol. 43, pp. 10317-10327, 2014.

[35] G. Fan, F. Li, D. G. Evans and X. Duan, "Catalytic applications of layered double hydroxides: Recent advances and perspectives," *Chemical Society Reviews,* vol. 43, pp. 7040-7066, 2014.

[36] M. Maroño, Y. Torreiro, L. Montenegro and J. Sánchez, "Lab-scale tests of different materials for the selection of suitable sorbents for CO2 capture with H2 production in IGCC processes," *Fuel,* vol. 116, pp. 861-870, 2014.

[37] Y. Tokudome, N. Tarutani, K. Nakanishi and M. Takahashi, "Layered double hydroxide (LDH)-based monolith with interconnected hierarchical channels: Enhanced sorption affinity for anionic species," *Journal of Materials Chemistry A,* vol. 1, pp. 7702-7708, 2013.

[38] H. Laguna, S. Loera, I. A. Ibarra, E. Lima, M. A. Vera and V. Lara, "Azoic dyes hosted on hydrotalcite-like compounds: Non-toxic hybrid pigments," *Microporous and Mesoporous Materials,* vol. 98, pp. 234-241, 2007.

[39] E. N. Kalali, X. Wang and D. .. Wang, "Functionalized layered double hydroxide-based epoxy nanocomposites with improved flame retardancy and mechanical properties," *Journal of Materials Chemistry A,* vol. 3, pp. 6819-6826, 2015.

[40] J. Sun, P. Li, J. Qu, X. Lu, Y. Xie, F. Gao, Y. Li, M. Gang, Q. Feng, H. Liang, X. Xia, C. Li, S. Xu and J. Bian, "Electricity generation from a Ni-Al layered double hydroxide-based flexible generator driven by natural water evaporation," *Nano Energy,* vol. 57, pp. 269-278, 2019.

[41] B. E. Warren, “X-Ray Diffraction in Random Layer Lattices,” *Phys. Rev.,* vol. 59, no. 9, pp. 693-698, 1941.

[42] M. Menetrier, K. S. Han, L. Guerlou-Demourgues and C. Delmas, “Vanadate-Inserted Layered Double Hydroxides: A 51V NMR Investigation of the Grafting process,” *Inorganic Chemistry,* vol. 36, pp. 2441-2445, 1997.

[43] H. Abdolmohammad-Zadeh and S. Kohansal, “Determination of mesalamine by spectrofluorometry in human serum after solid-phase extraction with Ni-Al layered double hydroxide as a nanosorbent,” *Journal of the Brazilian Chemical Society,* vol. 23, pp. 473-481, 2012.

[44] G. Abellan, E. Coronado, C. Marta-Gastaldo, A. Ribera and J. F. Sanchez-Royo, “Layered double hydroxide (LDH)-organic hybrids as precursors for low-temperature chemical synthesis of carbon nanoforms,” *Chemical Science,* vol. 3, pp. 1481-1485, 2012.

[45] A. M. Alansi, W. Z. Alkayali, M. H. Al-Qunaibit, T. F. Qahtan and T. A. Saleh, “Synthesis of exfoliated polystyrene/anionic clay MgAl-layered double hydroxide: Structural and thermal properties,” *RSC Advances,* vol. 5, pp. 71441-71448, 2015.

[46] P. Juhas, T. Davis, C. L. Farrow and S. J. L. Billinge, “3: a rapid and highly automatable program for processing powder diffraction data into total scattering pair distribution functions,” *Journal of Applied Crystallography,* vol. 46, pp. 560-566, 4 2013.

[47] H. M. Rietveld, “A profile refinement method for nuclear and magnetic structures,” *Journal of Applied Crystallography,* vol. 2, pp. 65-71, 6 1969.

5. Summary of other achievements not included above

The entirety of my scientific work is related to powder diffraction studies of various materials, each of which has potential technological applications. During my work, I developed my knowledge of various available diffraction methods while using X-rays, synchrotron radiation and neutrons. The base research method I have been using was powder diffraction. The results of most of the experiments were analysed by using the Rietveld method. Throughout the development of research methods, I have been using, I took part in various projects, and the experimental methods I used to analyse experimental data became more and more advanced.

Since the defence of my doctoral dissertation in 2009, I have published 15 papers in international journals (plus 7 indicated as the contents of this application), which is a total of 22 papers since 2010.

The first part of the published works is connected to the subject of my doctoral dissertation, i.e. the description of the atomic position and magnetic moments modulation and its relationships in $CaMnO_{12}$ and another related perovskite $CaCu_3Ti_4O_{12}$ (works **D10**, **D11**, **D12**, **D13**). The results described concerned the description of the modulated magnetic structure of $CaMnO_{12}$ at temperatures below 50 K. It is described by means of two propagation vectors, where magnetic moments of $Mn^{3+/4+}$ ions form a spiral in a plane perpendicular to the direction of the spiral propagation. Due to the presence of two modulation vectors, the overall value of the magnetic moment is not constant, but changes in a periodic way. Most of the above works have been published during my work as an adjunct in the group of Condensed Matter Structure headed by prof. Radosław Przeniosło at the Faculty of Physics, University of Warsaw.

During my first Postdoctoral position in the group of prof. H. Fjellvåg at the Faculty of Chemistry, University of Oslo (Norway), I started working on partially disordered materials (which is the subject of this application). At the same time, I took part in many powder diffraction experiments by using synchrotron radiation at European Synchrotron Radiation Facility (Grenoble, France), exploring new experimental possibilities: low and high temperature measurements, in-situ measurements, or in the presence of various gas atmospheres. As a result of this work, a number of papers describing crystalline materials from the family of zeolites were published, in particular concerning changes in the crystal structure during catalytic reactions (works **D2**, **D7**, **D8** and **D9**). The main goal throughout the work published in **D2**, **D8** and **D9** was the analysis of difference Fourier maps of electron density, searching for probable locations of Cu^{2+} ions and Mo_xC_y clusters. The work **D7** presents the analysis of the unit cell dimensions evolution as a function of location in the sample and time (a time and space resolved experiment).

Using a detailed analysis of the peak shape of Bragg maxima, including the use of non-analytical functions such as spherical harmonics, I determined the crystal structure in two materials: the ion conductor $La_4(Co_{1-x}Ni_x)_3O_{10+\delta}$ and the $BiMn_7O_{12}$ perovskite structure, as described in papers **D5** and **D6**, respectively.

My second Postdoctoral position was placed at ISIS Neutron and Muon Source (Didcot, Great Britain). My main responsibility was to prepare and develop a new version of the RMCProfile program (www.rmcprofile.org). RMCProfile is a computer program dedicate for the analysis of Pair Distribution Function (PDF). During that time, I significantly expanded my programming skills. I have also participated in several neutron powder diffraction experiments at the ISIS spallation source. As a result of my work, a new program has been created (some parts of the program have already been prepared by a previous programmer). This work was done in cooperation with research centres around the world (Oak Ridge National Laboratory in USA and Queen Marry University of London, Great Britain). While developing the algorithm for this program, it became necessary to derive mathematical expressions describing the PDF function in the case of multiphase systems, which was not known before. The result of this work was published in paper **D1**, where I am the sole author.

During my stay at the ISIS Neutron and Muon Source, I continued a collaboration with a group from the University of Oslo and the University of Warsaw (Faculty of Physics). As a result of this cooperation, I performed several powder diffraction neutron and synchrotron radiation experiments. As a result, publications **D4** and **D3** were published. In the work **D4**, the crystal structure of La_2LiHO_3, a new material from the *oxyhydrates* family, where the H^- ions occur, was described. Finally, in work **D3** the influence of the crystal size on the distortion of the cubic structure of Cr metal, was analysed.

Wojciech Stawiński